June 2023

WIDE-ANGLE LIQUID CRYSTAL POLARIZATION SWITCH

David Coleman
Meta Platforms Technologies, LLC

Gary D. Sharp
Meta Platforms Technologies, LLC

WIDE-ANGLE LIQUID CRYSTAL POLARIZATION SWITCH

By

David Coleman

and

Gary D. Sharp

WIDE-ANGLE LIQUID CRYSTAL POLARIZATION SWITCH

TECHNICAL FIELD

[0001] The present disclosure relates to polarization optical devices, and in particular to polarization-based optical switches, tunable optical modules, and visual displays using such polarization-based optical switches and tunable modules.

BACKGROUND

[0002] Visual displays provide information to viewer(s) including still images, video, data, etc. Visual displays have applications in diverse fields including entertainment, education, engineering, science, training, advertising, to name just a few examples. Some visual displays, such as TV sets, may display images to several users, while some visual display systems, such as near-eye displays (NEDs), are intended for use by individual viewers. NEDs wearable on the user's head may be self-contained, or may be connected to a controller or a console providing the video feed and/or required control functions.

[0003] An artificial reality system may include an NED (e.g., a headset or a pair of glasses) configured to present content to a user. The NED may display virtual objects or combine images of real objects with virtual objects in virtual reality (VR), augmented reality (AR), or mixed reality (MR) applications. For example, in an AR system, a user may view images of virtual objects (e.g., computer-generated images) superimposed with the surrounding environment by seeing through a "combiner" component. The combiner of a wearable display is typically transparent to external light but includes some light routing optic to place the display-generated images into the user's field of view.

[0004] Because an HMD is worn on the head of a user, a large, bulky, unbalanced, and/or heavy display device would be cumbersome and uncomfortable for the user to wear. Consequently, head-mounted display devices can benefit from a compact and efficient configuration, including efficient light sources providing illumination of a display panel, high-

throughput ocular lenses, reflectors, diffractive optical elements, polarization switches and beam redirectors, varifocal lenses, and other optical elements in the image forming train.

BRIEF DESCRIPTION OF THE DRAWINGS

[0005] Exemplary embodiments will now be described in conjunction with the drawings, in which:

[0006] FIG. 1 is a Poincaré sphere view of a polarization transformation by a mixed twisted nematic (MTN) liquid crystal (LC) cell for red, green, and blue light;

[0007] FIG. 2 is a Poincaré sphere view of a polarization transformation by a matched pair of MTN LC cells with opposite twist directions for the red, green, and blue light;

[0008] FIGs. 3A and 3B are schematic views of a polarization switch of this disclosure in first (FIG. 3A) and second (FIG. 3B) switching states;

[0009] FIG. 4 is a Poincaré sphere view of a polarization transformation by a passive compensation structure (PCS), or a dispersive polarization rotator, of the polarization switch of FIGs. 3A and 3B;

[0010] FIG. 5 is a Poincaré sphere view of a polarization transformation by a PCS including a stack of uniaxial quarter-wave (QW) layers;

[0011] FIG. 6 is a Poincaré sphere view of a polarization transformation by a PCS including a stack of biaxial QW layers;

[0012] FIGs. 7A and 7B are schematic stack diagrams of a polarization switch of this disclosure for converting a linear polarization (LP) into a left-hand circular polarization (LHCP; FIG. 7A) and a right-hand circular polarization (RHCP; FIG. 7B) using the PCS of FIG. 5;

[0013] FIGs. 8A and 8B are Poincaré sphere views of polarization transformations by the polarization switch of FIGs. 7A and 7B, respectively;

[0014] FIGs. 9A and 9B are schematic stack diagrams of a polarization switch of this disclosure for converting LP into LHCP (FIG. 9A) and RHCP (FIG. 9B) using the PCS of FIG. 6;

[0015] FIGs. 10A and 10B are contrast polar plots for the linear-to-circular polarization transformation by the polarization switch of FIGs. 9A and 9B respectively;

[0016] FIGs. 11A and 11B are schematic stack diagrams of a polarization switch of this disclosure for converting LP into LHCP (FIG. 11A) and RHCP (FIG. 11B);

[0017] FIG. 12 is a Poincaré sphere view of the polarization transformation by a circular-to-linear PCS of the polarization switch of FIGs. 11A and 11B, the PCS including a five-layer $0R_{th}$ QW stack, forming a quarter-wave retarder with dispersive rotation;

[0018] FIGs. 13A and 13B are contrast polar plots for the circular-to-circular polarization transformation by the polarization switch of FIGs. 11A and 1B respectively;

[0019] FIG. 14 is a flow chart of a method for constructing a polarization switch of this disclosure;

[0020] FIG. 15 is a flow chart of a method for configuring a polarization switch of this disclosure;

[0021] FIG. 16A is a frontal view of a Pancharatnam–Berry phase **(**PBP) LC lens as an example polarization-switchable element of this disclosure;

[0022] FIG. 16B is a magnified schematic view of LC molecules in an LC layer of the PBP LC lens of FIG. 16A;

[0023] FIG. 17 is a side schematic view of the PBP LC lens of FIG. 16A illustrating light propagation depending on handedness of circular polarization of impinging light;

[0024] FIG. 18A is a frontal view of a PBP LC grating as an example polarization-switchable element of this disclosure;

[0025] FIG. 18B is a magnified schematic view of LC molecules in an LC layer of the PBP LC grating of FIG. 18A;

[0026] FIG. 19 is a side schematic view of the PBP LC grating of FIG. 18A illustrating light propagation depending on handedness of circular polarization of impinging light;

[0027] FIG. 20 is a top cross-sectional view of an augmented reality (AR) display of this disclosure having a form factor of a pair of eyeglasses; and

[0028] FIG. 21 is a three-dimensional view of a head-mounted display (HMD) of this disclosure.

DETAILED DESCRIPTION

[0029] While the present teachings are described in conjunction with various embodiments and examples, it is not intended that the present teachings be limited to such embodiments. On the contrary, the present teachings encompass various alternatives and equivalents, as will be appreciated by those of skill in the art. All statements herein reciting principles, aspects, and embodiments of this disclosure, as well as specific examples thereof, are intended to encompass both structural and functional equivalents thereof. Additionally, it is intended that such equivalents include both currently known equivalents as well as equivalents developed in the future, i.e., any elements developed that perform the same function, regardless of structure.

[0030] As used herein, the terms "first", "second", and so forth are not intended to imply sequential ordering, but rather are intended to distinguish one element from another, unless explicitly stated. Similarly, sequential ordering of method steps does not imply a sequential

order of their execution, unless explicitly stated. In FIGs. 3A-3B, 7A-7B, 9A-9B, and 11A-11B, similar reference numerals denote similar elements.

[0031] Polarization switches based on switchable half-wave plates have intrinsic wavelength dependence of the output SOP because a half-wave optical retardation for green light is more than half-wave optical retardation for blue light having a shorter wavelength than the green light, and is less than half-wave optical retardation for red light having a longer wavelength than the green light. For LC-based switchable half-wave plates, the issue is further exacerbated by the fact the LC devices typically respond to an applied voltage by rotating the polarization axis to align with the applied electric field, which in most cases increases a thickness-direction retardation responsible for variation of optical performance of the polarization switch with angle of incidence.

[0032] In accordance with this disclosure, a polarization switch may employ a pair of LC cells operating in counter-phase, i.e. when one LC cell is ON (i.e. is in the driven or high-voltage state), the other LC cell is OFF (i.e. in the undriven or low-voltage state), and vice versa. In such a configuration, the thickness-direction retardation is substantially independent on the switching state, and thus may be passively compensated by an appropriate fixed retarder. A passive compensation structure (PCS) is provided to convert the input polarization state to the first polarization state together with the first LC cell in the undriven state, and to convert the input polarization state to the second polarization state together with the second LC cell in the undriven state. The PCS may be configured to convert the input polarization of a plurality of spectral components of impinging light to mid-way polarization states wavelength-dispersed along a mid-way plane between the first and second polarization states on a Poincaré sphere, to compensate for, or offset, an inherent wavelength dependence of polarization transformation of a corresponding LC cell in the undriven state.

General Considerations for Achromatic Polarization Switching

[0033] This disclosure pertains to liquid crystal (LC) based polarization switching devices that transform an input state of polarization (SOP) to two or more output SOPs. It may be desirable to transform a wavelength-independent SOP to two or more substantially achromatic

output SOPs. These SOPs may be linear polarizations of any orientation, circular polarizations (left-handed or right-handed), or any set of elliptical SOPs with arbitrary ellipticity, orientation, and handedness. For visual display applications, it may be desirable to make the performance of the switch achromatic over a visible wavelength range.

[0034] The collective action of the elements of a polarization switch of this disclosure may be to create wavelength-specific polarization paths, such that the endpoints on the Poincaré sphere are coincident for a prescribed spectral bandwidth. This represents an embodiment of engineered reverse polarization dispersion, where two or more elements cooperate to create Poincaré sphere paths that are wavelength specific. Spectral diversity in Poincaré sphere paths can compensate for the wavelength dependence of the length of the path, permitting a range of wavelengths to converge virtually to the same endpoint on the Poincaré sphere. In the switch configuration disclosed herein, this represents a "composite" polarization transformation that relies on the action of LC devices and passive compensation structures (PCSs). The PCSs may be optimized to provide a minimal separation between the target SOP and each endpoint on the Poincaré sphere. The optimization may average this separation over a prescribed range of wavelengths, possibly with spectral (e.g. photopic) weighting.

[0035] This disclosure further pertains to achromatic polarization switching that aims to lessen sensitivity of the output SOP to incidence angle in each of the two or more states. Specifically, the achromatic in-plane performance is preferably maintained as the incidence angle increases relative to normal. This may be accomplished using an active compensation scheme, where cells are driven out of phase to create a static thickness-direction retardation in both states. The LC devices may be similar in construction, or even identical, while providing unique in-plane functionality, such that passive compensation improves the off-axis performance of both states. Field of view compensation may be incorporated into the PCS, or it may be between or adjacent to the two or more LC devices.

[0036] The input SOP may be arbitrarily oriented linear (e.g. from a conventional broadband visual display linear polarizer), with the outputs being achromatic left-hand circular polarization (LHCP), and achromatic right-hand circular polarization (RHCP). In this case, the PCS in-plane function may be to pre- (or post-) condition the SOP, e.g. transforming the achromatic linear

input to a wavelength-dependent linear orientation. The LC devices may then transform the wavelength-dispersed linear SOP to a common circular SOP.

[0037] The input SOP may be achromatic e.g. LHCP provided by a range of devices with broadband circular eigen-polarizations (e.g. a cholesteric LC device, a circular polarizer, or a Pancharatnam Berry Phase (PBP) diffractive element), with the outputs being achromatic LHCP and achromatic RHCP. In this instance, the switching structure may optimally leave the input SOP unchanged in one voltage state, while the input is transformed to the orthogonal SOP in another voltage state of the LC devices. The PCS may be required to convert the achromatic circular SOP to a wavelength-dispersed linear SOP in this instance.

[0038] The switching device may be operated in reverse, such that a pair of achromatic input SOPs may be light-efficiently converted to a common output SOP. For example, one voltage state of the switching device may convert an input LHCP to an arbitrarily oriented achromatic linear SOP, while a second voltage state may convert an input RHCP to the same output linear output SOP. A linear polarizer may be added to output an achromatic and uniform linear polarization state.

[0039] A switching structure of this disclosure may consist of several polarization control elements, both passive and active. Active devices may be LC cells, and passive devices may be retarders with a prescribed in-plane and thickness-direction phase difference or retardation. The in-plane retardation values, orientations and eigen-polarizations may be selected to facilitate a set of "composite" polarization transformations that represents e.g. a pair of achromatic output SOPs. These outputs may represent orthogonal (e.g. linear or circular) SOPs with wavelength independence.

[0040] LC devices include zero-twist nematic types, such as anti-parallel aligned electrically-controlled-birefringence (ECB), parallel-aligned pi-cell, vertically-aligned (VA), and hybrid configurations. They further include arbitrary twisted nematic (TN) configurations, such as 45° TN, 60-70° TN, 90° TN, or super-twist nematic alignment, and twisted VA modes. The LC devices considered herein may further include in-plane LC devices, such as ferroelectric liquid crystal (FLC) and in-plane-switched (IPS) nematics.

[0041] Nematic LC devices (e.g. an ECB or TN device) may be operated in a binary mode, such that a desired polarization transformation is produced in the non-energized state (e.g. 0V), with no polarization transformation produced in the fully energized state (e.g. 20V). An exemplary transformation in the non-energized state may be to convert an input SOP to an intermediate output SOP, e.g. linear to circular polarization, for all relevant wavelengths. This may further call for the device to behave as a functionally isotropic element in the fully energized state. The former may be difficult to achieve over a broad range of wavelengths (due to the wavelength dependence of retardation), while the latter may be relatively straightforward to achieve.

[0042] It is convenient to describe the behavior of a nematic LC device in terms of the in-plane distribution of the LC director and the thickness-direction distribution of the LC director. The former determines the functional polarization transformation near normal incidence, while the latter can introduce distortion in the transformation as the incidence angle grows. Exemplary switch devices of this disclosure may be operated in a binary mode, such that the director field is substantially in-plane in the functional or undriven state, and substantially normal to the device in the alternate, i.e. fully energized or driven state. In practice, the extent of the oblique director tilt near the boundary may be lessened by using low pretilt alignment layers, and by operating the LC cell at sufficiently high driving voltage. The functional or undriven state may use a sufficiently low driving voltage, i.e. the undriven state may be achieved at a low driving voltage that may be fine-tuned to provide optimal performance in the functional state.

[0043] In an idealized condition, an entirely in-plane director field produces an achromatic transformation in the functional state. Assuming a uniaxial LC, the cell can be described as having an in-plane retardation of

[0044] $$R_e = R_0 = \left(n_x - n_y\right)d = (n_e - n_o)d = \Delta n d \qquad (1)$$

[0045] where n_e is the extraordinary refractive index, n_o is the ordinary refractive index, d is the cell gap, and Δn is the wavelength-dependent birefringence. This is the total retardation (or pathlength difference) of the cell, though the director field could have a twisted arrangement. If

the LC cell has a zero twist angle, it can be considered an "A-Plate". An A-Plate also has a thickness-direction retardation given by

[0046] $$R_{th} = \left[\left(\frac{n_x+n_y}{2}\right) - n_z\right] d = R_0/2 \quad (2)$$

[0047] In practice, non-zero thickness-direction retardation R_{th} tends to limit the performance of the LC cell as the incidence angle increases relative to normal. Were R_{th} instead zero, the in-plane functionality of the LC cell could be substantially preserved with incidence angle.

[0048] In another idealized condition, the director field of the fully energized LC is virtually normal to the device, forming a virtual +C plate. For this example,

[0049] $$R_e = 0 \quad (3)$$

and

[0050] $$R_{th} = -R_0 \quad (4)$$

[0051] At normal incidence, the projection of the director field onto the plane of the device is in general zero, so it is functionally isotropic. However, the large negative R_{th}, or +C Plate retardation, introduces off-normal retardation that can degrade device performance.

[0052] The above illustrates the important fact that modulation of an in-plane retardation, whether twisted or not, is coupled with a modulation of the thickness-direction retardation. For the ECB example, which is closely related to the VA example, an in-plane modulation of R_0 is coupled with a net thickness direction modulation of $3R_0/2$. An objective of this disclosure is to identify structures that produce an achromatic modulation of the in-plane polarization transformation, while minimizing the thickness-direction retardation in any set of voltage states. In a preferred embodiment, a switching symmetry is used, such that the overall R_{th} is in general zero.

[0053] The above shows that, with a sufficient driving voltage, the virtual +C plate represents an achromatic state near normal incidence, as would be expected for an element that is functionally isotropic. However, achieving an achromatic transformation in the non-energized state is more challenging. With A-Plate behavior, for example, converting broadband light from e.g. LHCP to RHCP requires an achromatic half-wave of phase retardation. That is,

[0054] $$\Gamma = \pi = \frac{2\pi R_0}{\lambda} \quad (5)$$

[0055] which gives the well-known reverse-dispersion requirement, or $d\Delta n(\lambda) = \lambda/2$. That is, the birefringence must increase linearly with wavelength λ to produce wavelength-independent transformations. In practice, active LC materials tend to have positive birefringence dispersion that further exacerbates the wavelength-dependence of a transformation.

[0056] In the absence of a reverse-dispersion LC material, the present disclosure seeks to identify composite transformations that synthesize such an achromatic transformation. In this context, a composite transformation is the result of contributions from two or more polarization-functional elements. Examples of engineered reverse-dispersion elements include compound retarders, e.g. Pancharatnam quarter-wave (QW)/half-wave (HW), Koester rotators, and pure achromatic rotators disclosed by Sharp in U.S. Patent No. US 8,408,708, filed on May 21, 2010 and incorporated herein by reference in its entirety. Such structures can be configured to act on any input SOP, most commonly a linear or circular input. In some embodiments, the structure provides an achromatic HW of retardation when operating on an input circular SOP, converting from LHCP (RHCP), to RHCP (LHCP). Twisted passive and active elements can also be used to create embodiments of this disclosure.

[0057] As noted above, the two LC cells may be driven anti-phase, such that one cell is driven to the +C plate state while the other provides an in-plane function (State 1), and vice versa (State 2). Because of the symmetry of the switching, the composite R_{th} value is constant in driving between the two states, so it can be passively compensated. The two in-plane functions are distinct, such that an effective sum-difference retardation is produced when the cells are combined with a passive in-plane bias retarder (or retarder stack). Because active compensation

requires cells that switch only half of the total retardation, switching speed can be much faster. For example, a half-wave liquid crystal cell in a conventional single-switch configuration, can be replaced by a pair of cells each with a quarter-wave of retardation. Because the relaxation time of an LC device is proportional to the square of the cell gap, QW cells can switch four-times faster than HW cells using the same LC material. Examples of active compensation are given for linear to quasi-linear switching using linear retarders. Performance of the half-wave state may be limited by the dispersion of the retarders in the examples shown.

[0058] Examples disclosed herein cover additional wide-angle, achromatic switching using active compensation, with specific configurations of LC cells and passive structures, to produce achromatic polarization transformations for two or more states. The switches may provide transformations that are e.g. linear-to-circular, linear-to-linear, circular-to-circular, or circular-to-linear. The switches may incorporate passive or active LC twisted structures to accomplish these transformations.

Passive Compensation Structure

[0059] In an active compensation configuration where a pair of cells is driven anti-phase, only one cell participates in the polarization transformation in any voltage state. Furthermore, it may be preferable to use pairs of LC cells that may have similar functional parameters such as R_0 and twist angle, but different specific in-plane function. This enables a balanced R_{th} in each state, and therefore a switch that can be optimally compensated for operation over a wide field of view. In this scenario, the input SOP may be accounted for by defining additional transformations that facilitate specific outputs.

[0060] According to an aspect of this disclosure, a passive compensation structure (PCS) is provided to facilitate optimal transformations between an input SOP and two orthogonal output SOPs. This may refer to transformations that are wavelength-independent over a prescribed spectral band, e.g. 400nm – 700nm. The PCS has in-plane functionality, but may also have a thickness-direction retardation for improving the field-of-view performance. With respect to the light path, the PCS can precede the LC devices, follow the LC devices, or in more rare cases be disposed between the devices. In general, the PCS transforms the SOP by creating two or more

waves using birefringence, introducing phase differences, and recombining them along a common path. The eigen-polarizations of the PCS building blocks can be linear retarders, circular retarders, and/or elliptical retarders, for example. The PCS eigen-polarizations may be wavelength-stable, or they may be wavelength-dependent. The PCS can be a compound element, composed of stacks of engineered layers.

[0061] The functional requirements of the PCS depend upon specifics of the input and output states of the switch. For instance, if the input SOP is identical to one of the outputs, then the PCS may provide a transformation that biases the SOP to a substantially intermediate state. Considering the Poincaré sphere, if the input is circularly polarized and the outputs are circularly polarized, the PCS may bias the SOP to the equator (i.e. linear SOPs). In this example, the bias represents substantially one quarter-wave of retardation. If the input is linear (e.g. oriented at 0 degrees) and the outputs are linear (oriented at 0 and 90 degrees), the PCS may bias the SOP to an elliptical state with axis rotated by $\pm 45°$. If the system permits it, this may be accomplished by rotating the input linear polarizer to $\pm 45°$ with respect to the outputs. According to an aspect of this disclosure, the PCS may transform the input to lie substantially on a Poincaré mirror-plane between the two outputs, i.e. on a plane equidistant from both output polarization states, to enable active compensation.

[0062] If the input is linear (circular) and the outputs are circular (linear), no such bias may be required. However, there is usually a secondary functional requirement of the PCS, which is that it account for dispersion requirements needed to ensure that wavelengths of interest all map to a common endpoint. Composite transformations of this disclosure are substantially achromatic, and these are optimally accomplished through the combined action of, and cooperation between, the PCS and the specific LC device. An important characteristic of twisted LC devices is that the transformation path on the Poincaré sphere is a function of both input SOP and wavelength.

[0063] A twisted LC device has a degree of freedom not possessed by a linear retarder device, e.g. an electrically-controlled birefringence (ECB) device. In typical positive dispersion A-Plates, the Poincaré transformation path is wavelength-independent, but the arc length

decreases with increasing wavelength. This makes it impossible for the endpoint from a single device to be achromatic. Conversely, a single twisted structure can provide unique paths for each wavelength, providing a greater degree of freedom for engineering a required wavelength dispersion of polarization transformation.

[0064] A Poincaré sphere view of FIG. 1 provides a non-limiting illustrative example of a polarization transformation by an MTN LC cell for red (R), green (G), and blue (B) wavelengths of 650nm, 550nm, and 450nm respectively, assuming an achromatic circularly polarized input at a top of a Poincaré sphere 120. Herein and throughout the rest of the specification, the term "MTN" means that the angle of twist may be different from a typical value of 90 degrees used in liquid crystal displays. In the specific example of FIG. 1, the twist angle of the MTN LC cell is 68°, and the retardation is 235nm at a wavelength of 550nm. The circularly polarized input at the top of the Poincaré sphere 120 maps to a quasi-linearly polarized output at its equator 122, where the orientation of linear polarization, given by an azimuthal position of the R, G, and B end points near the equator of the Poincaré sphere, is a function of wavelength, $\theta(\lambda)$. The polarization transformation of red (R), green (G), and blue (B) light is illustrated in FIG. 1 with dashed, solid, and dash-dotted curves respectively.

[0065] The ellipticity field ratio and orientation are given in Table 1 below. This also shows the converse, which is that a quasi-linear input with wavelength-dependent orientation $\theta(\lambda)$ maps to an achromatic circular SOP. Either way, this transformation represents approximately a quarter-wave of retardation at each wavelength, i.e. it represents an embodiment of a reverse dispersion. FIG. 1 also illustrates the deficiencies of a single MTN LC cell, in that the SOP does not perfectly map between pole and equator of the Poincaré sphere. The red endpoint (R) is north of the equator (i.e. less than a QW), and the green endpoint (G) is south of the equator (i.e. over a QW). Therefore, while it does possess a measure of reverse dispersion relative to a linear retarder, an MTN LC cell may be not a perfect reverse-dispersion quarter-wave retarder over the entire spectral band of visible light.

Table 1. Output of a single MTN and a pair of MTN cells with reverse-twist symmetry.

Wavelength	Orientation (single)	Ellipticity (single)	Ellipticity (pair)
Red (650nm)	21.0°	0.038	0.854
Green (550nm)	13.6°	0.034	0.865
Blue (450nm)	0.2°	0.008	0.927

[0066] FIG. 2 illustrates that pairing of the MTN LC cell of FIG. 1 with the second MTN LC cell matching the first MTN LC cell but having a reverse twist direction enables one to obtain a quasi-achromatic handedness change of a circular polarization of impinging light. That is, the matched MTN LC cell pair is functionally an approximate half-wave retarder for circularly polarized light. The wavelength dependence of the polarization transformation path on the Poincaré sphere 120 of FIGs. 1 and 2 causes the polarization of blue light to undergo a more tortuous path on the Poincaré sphere than the red light, as required to compensate for retardation dispersion.

[0067] For a circular polarization handedness switch using MTN LC cells in an active compensation configuration, one of the FIG. 2 transformations may be provided by a PCS. This could be accomplished e.g. by simply using a fixed twisted structure matched to the MTN LC cell with reverse twist symmetry. In principle, the transformation may look exactly like that of FIG. 2. More generally though, this disclosure includes any PCS that delivers the required input-to-output transformation, regardless of the route taken on the Poincaré sphere 120. A PCS composed of a stack of linear retarders can map an achromatic linear SOP to the wavelength dispersed angle θ of linear SOP, $\theta(\lambda)$, on an equator 122 of the Poincaré sphere 120, as required by the specific MTN cell. Alternatively, the PCS retarder stack could be configured to map an achromatic circular SOP to the wavelength dispersed linear SOP. Such a stack can have an arbitrarily close match to the specific LC birefringence dispersion. This can be a beneficial aspect of polarization switch configurations considered in this disclosure, in that no material with an exotic dispersion behavior is required for a PCS of this disclosure, making it possible to achieve an arbitrarily close match to LC dispersion using a stack of materials with a common dispersion.

Example Polarization Switch Configurations

[0068] Referring to FIGs. 3A and 3B, an exemplary polarization switch 300 of this disclosure converts an input achromatic polarization state 301 of impinging light 302 into one of two output mutually orthogonal achromatic polarization states, 321A (FIG. 3A) or 321B (FIG. 3B). In FIG. 3A, the first LC cell 311 is in the undriven or low-voltage state (white rectangle) having a non-zero in-plane retardation, while the second LC cell 312 is in the driven or high-voltage state (shaded rectangle) having a substantially zero in-plane retardation. In FIG. 3B, the first LC cell 311 is in the driven or high-voltage voltage state (shaded rectangle) having a zero in-plane retardation, while the second LC cell 312 is in the undriven or low-voltage state (white rectangle) having a non-zero in-plane retardation.

[0069] The impinging light 302 has a plurality of spectral components, in this example a red spectral component 302R, a green spectral component 302G, and a blue spectral component 302B. A PCS 304 converts the input polarization state 301 of the red 302R, green 302G, and blue 302B spectral components of the impinging light 302 to a wavelength-dispersed intermediate polarization state 303. The polarization state imparted by the PCS 304 onto the multi-color impinging light 302 is optimized to match the wavelength-dependent polarization transformation of first 311 and second 312 LC cells when in the undriven state, from the first 321A and second 321B output polarization states respectively. As a result of the polarization transformation matching, the input polarization state 301 may be converted to the first output polarization state 321A by the combination of the PCS 304 and the first LC cell 311 in the undriven state (FIG. 3A), and to the second output polarization state 321B by the combination of the PCS 304 and the second LC cell 312 in the undriven state (FIG. 3B). The other LC cell is accordingly in the driven state that erases the in-plane performance, i.e. has a substantially zero in-plane retardation, and thus does not perturb the polarization transformation achieved by the combination of the PCS 304 and the undriven LC cell.

[0070] The polarization switch 300 may further include a controller 350 operably coupled to the first 311 and second 312 LC cells. To convert the input polarization state 301 into the first output polarization state 321A, the controller 350 may be configured, e.g. programmed, hardwired, etc., to drive the second LC cell 312 to the high-voltage state while having the first

LC cell 311 in the undriven or low-voltage state. By the same token, to convert the input polarization state 301 into the second output polarization state 321B, the controller 350 may be configured to drive the first LC cell 311 to the high-voltage state while having the second LC cell 312 in the low-voltage state. Driving the first or second LC cell to the high-voltage state may include e.g. applying a first voltage to the first or second LC cell respectively. Similarly, having the first or second LC cell in the undriven or low-voltage state may include applying a second voltage to the first or second LC cell respectively, the second voltage being lower than the first voltage. The first and second output polarization states may be substantially achromatic.

[0071] A specific example of configuration of the polarization switch 300 will now be discussed. Referring back o FIGs. 1, 2 while still referring to FIGs. 3A and 3B, the input polarization state 301 and the first output polarization state 321A (FIG. 3A) may be the "achromatic circular input" at the top of the Poincaré sphere of FIGs. 1 and 2, and the second output polarization state 321B (FIG. 3B) may be the "quasi-achromatic output" at the bottom of the Poincaré sphere (FIG. 2). In this example, the PCS 304 provides the initial polarization transformation presented in FIG. 1, the first LC cell 311 provides a transformation reverse w.r.t. the one of FIG. 1, and the second LC cell 312 provides a second transformation of FIG. 2, which transforms from the wavelength-dispersed linear polarization at the equator of the Poincaré sphere in FIG. 2 to the bottom "quasi-achromatic output" in FIG. 2. The imperfection of a TN/MTN LC cell performance in failing to map all wavelengths exactly to the equator of the Poincaré sphere is exacerbated when paired with a (M)TN LC cell having substantially same parameters other than a twist direction or twist symmetry, as illustrated in FIG. 2. This is clear by observing the separation of R, G, and B endpoints near the south pole of the Poincaré sphere in FIG. 2, and from Table 1 above, where ellipticity is lower in the red and green part of the visible spectrum.

[0072] The output ellipticity, or more generally a deviation from a target polarization state, of red, green, and blue light may be balanced out by a further optimization of the PCS 304, allowing one to achieve a substantially achromatic performance for both output polarization states 321A, 321B and all spectral components within a spectral band of the impinging light 302. By way of non-limiting examples, the spectral components of the light in the first and/or second

polarization state may be within 10 degrees, 15 degrees, or 30 degrees from one another on the Poincaré sphere. Herein and throughout the specification, the term "substantially achromatic" or "quasi-achromatic" denotes achromaticity to at least within 30 degrees distance between different color components of the impinging light on Poincaré sphere.

[0073] The examples of FIGs. 1 and 2 provide a transformation from one circular polarization to another. More generally, the input polarization state may be any polarization state, and the PCS 304 may be configured to provide a polarization transformation from that initial polarization state to a wavelength-dispersed intermediate state 303. The first 321A and second 321B output polarization states may be any two mutually orthogonal, substantially achromatic polarization states on a Poincaré sphere. This is illustrated in FIG. 4 showing a Poincaré sphere 420 with right-hand circular polarization (RHCP) at the top and left-hand circular polarization (LHCP) at the bottom of the Poincaré sphere. The equator of the Poincaré sphere 420 is not shown in FIG. 4 for simplicity. The PCS 304 may convert an input polarization state 401 of the red 302R, green 302G, and blue 302B spectral components (FIGs. 3A and 3B) to mid-way polarization states 403R, 403G, and 403B respectively (FIG. 4). The conversion is illustrated with three solid curved arrows extending from the input polarization state 401 to the respective polarization states 403R, 403G, and 403B.

[0074] The mid-way polarization states 403R, 403G, and 403B are wavelength-dispersed on the Poincaré sphere 420 along a line 409 of intersection of the Poincaré sphere 420 with a mid-way plane 410, or a "mirror plane", between orthogonal first 411 and second 412 output polarization states on the Poincaré sphere 420. The mid-way plane 410 is equidistant from the first 411 and second 412 output polarization states and perpendicular to a line 414 connecting the first 411 and second 412 output polarization states on the Poincaré sphere 420. The PCS 304 may be configured to offset a wavelength dispersion of the in-plane retardation of either one of the first 311 or second 312 LC cells in the undriven state within a spectral bandwidth of the plurality of spectral components e.g. red, green, and blue spectral components, which may occupy a wavelength range of e.g. between 400nm and 700nm.

[0075] One consideration in configuring a PCS is that it is may be impossible to passively compensate for deficiencies in the LC cell transformations that occur in both output states. For

example, if the PCS is configured to compensate for the ellipticity shown in FIG. 1, perfect circular polarization can be delivered in State 1 (same as "Achromatic Circular Input", top of FIG. 2). When the MTN LC cells are switched, the effect of that compensation is to degrade the performance of State 2 ("Quasi-Achromatic Output", bottom of FIG. 2). If one output state is of a higher importance than the other, this can be incorporated into a desired polarization switch configuration. In other embodiments, the optimization may be based on a balanced performance in both states. This means that the PCS configuration optimally maps the input polarization to the Poincaré sphere mirror plane to accommodate an achromaticity requirement of the first and second output polarization states.

Example Implementations of PCS and Polarization Switch

[0076] FIG. 5 shows a Poincaré sphere mapping of a 5-layer PCS using a cyclic-olefin-polymer (COP) with 130nm of retardation. Such a PCS may be useful for a switch that accepts a linear input polarization 501, and outputs a circular polarization with switchable handedness at the top and bottom of the Poincaré sphere 120. The polarization paths of red, green, and blue light are shown with dashed, solid, and dash-dotted lines, respectively, with the consecutive action of each subsequent layer of the 5-layer PCS denoted with respective numerals (1), (2), (3), (4), and (5). The dispersive rotation angle, $\theta(\lambda)$, of an MTN cell was used to define the desired PCS output SOP denoted with (R), (G), and (B) along the equator 122 of the Poincaré sphere 120. To balance the performance in each state, the target PCS output was linear polarization. In other words, the residual ellipticity introduced by an MTN LC Cell was not accounted for.

[0077] A global minimizer algorithm has been used to identify a retarder stack with an optimized performance. The optimization criteria may be based e.g. on leakage of the orthogonal polarization averaged over angle of incidence (e.g. 0° – 30°), azimuthal angle (e.g. 0° – 360°), and wavelength (e.g. 440nm – 650nm). The optimization procedure may use a sparse set of wavelengths (e.g. 440 nm, 550 nm and 650 nm) covering the wavelength range. For each wavelength and incidence angle, the leakage power oriented along $\theta(\lambda) + \pi/2$ can be calculated. Configurations that minimize global leakage over the range of wavelengths and incidence angles may possess an intrinsically low composite R_{th}, even though the stack may be

composed of uniaxial materials. FIG. 5 shows the transformations for a 5-layer configuration based on uniaxial retarders, where minimizing composite R_{th} is incorporated into the stack configuration.

[0078] FIG. 6 shows a similar Poincaré sphere polarization transformations for a PCS configuration based on the same (130nm) in-plane retarder, but with each layer having a zero R_{th}, denoted herein as $0R_{th}$. Because the stack is composed of layers with inherent insensitivity to incidence angle, the angles differ from those of FIG. 5. The notations of the polarization transformation paths are the same as in FIG. 5. It is to be noted that the FIG. 6 configuration de-emphasizes the transformations from the first QW layers, versus those of FIG. 5.

Field of View Compensation

[0079] According to the active compensation principle employed herein, the LC Cell 2 may be driven to a +C plate state while the LC Cell 1 has a first in-plane function in State 1, and the LC Cell 1 may be driven to a +C plate cell while the LC Cell 2 has a second in-plane function in State 2. A -C plate may be disposed between the LC cells 1 and 2 that compensates for the +C plate retardation introduced by the LC cell that is in the driven state. The central location of the -C plate ensures that the composite R_{th} can be nullified in both states because the compensator is always directly adjacent to an energized LC cell. In addition, the -C plate retardation may be adjusted downward if it also contributes to compensating the +C plate retardation contributed by the undriven LC cell (i.e. the LC cell in the functional state). The effectiveness of the C plate compensation on the undriven LC cell depends upon the azimuth distribution of R_{th} associated with the specific LC device. For MTN devices, which exhibit azimuth-dependent R_{th}, the azimuth independent compensation of the C plate may be only partially effective.

[0080] Passive FOV compensation is enabled by a polarization switch configuration with a composite R_{th} that is independent of the voltage state. The residual composite R_{th} may be subtracted off using practical compensation schemes, such as ±C plates, or ±A-Plates. For instance, crossed +A-Plates can act as an azimuth-dependent -C plate. The effect of specific compensators also depends upon the input SOP. By way of a non-limiting example, a C plate

introduces an azimuth-dependent retardation for a linear input SOP, but it introduces azimuth independent retardation for a circular input. As such, both the compensator type and position in the polarization switch stack may be important.

[0081] Common positive uniaxial retarders, whether twisted or untwisted, have a positive R_{th} and therefore may benefit from a compensator with a negative R_{th}. Though less common, negative uniaxial retarders also exist, e.g. discotic reactive mesogen LCP, or stretched polystyrene, and can be incorporated into a PCS configuration. If the PCS is composed of positive uniaxial retarders, preferred stack configurations (i.e. the arrangement of slow-axis for each retarder in the stack) accomplish the required in-plane functionality, while providing practical compensation configurations. For instance, a stack with an azimuth-independent composite R_{th} at the output is more easily compensated with a single +C plate with offsetting retardation. This is more practical than e.g. adding R_{th} compensators between the layers of the PCS. Exemplary PCS configurations may have self-compensating composite R_{th}. A PCS composed of a stack of biaxial base retarders satisfying $n_z = (n_x + n_y)/2$, is exemplary in that it provides polarization transformations that are substantially incidence-angle independent, regardless of the specific layout of slow axes.

Example 1: Linear-to-Circular Switch Using Uniaxial PCS and MTN LC Cells

[0082] Referring to FIGs. 7A and 7B, a polarization switch 700 is an embodiment of the polarization switch 300 of FIGs. 3A and 3B, includes similar elements, and operates by a similar principle. The polarization switch 700 converts an input polarization state of impinging light 702, e.g. a linear polarization state defined by an optional input polarizer 705, into one of mutually orthogonal first or second output polarization states. The output polarization states are left-hand circular polarization (LHCP; FIG. 7A) and right-hand achromatic circular polarization (RHCP; FIG. 7B). The LHCP and RHCP states may be substantially achromatic over a spectral width of visible light, or at least over 450nm – 650nm wavelength range.

[0083] The polarization switch 700 of FIGs. 7A and 7B includes a stack of the following layers: a PCS 704, first 711 and second 712 MTN LC cells, and a compensator plate 715

between the first 711 and second 712 MTN LC cells. The first 711 and second 712 MTN LC cells have a non-zero in-plane retardation in an undriven or low-voltage state. In a driven or high-voltage state, the first 711 and second 712 MTN LC cells have a near-zero in-plane retardation, and a maximum thickness-direction retardation R_{th}. The first LC cell 711 has a 68° twist angle, going from 158° to 90°. The second LC cell 712 has a 68° twist angle, going from 68° to 0°.

[0084] The PCS 704 is configured to convert the input polarization state to the first polarization state together with the first LC cell 711 in the undriven state and the second LC cell 712 in the driven state. The PCS 704 is further configured to convert the input polarization state to the second polarization state together with the second LC cell 712 in the undriven state and the first LC cell 711 in the driven state. To provide the stated polarization transformations, the PCS 704 includes a stack of fixed retarders 714, in this embodiment a stack of +A type retarders. Herein and throughout the rest of the specification, the term "+A type retarder" means a uniaxial retarder having an extraordinary refractive index larger than the ordinary refractive index, with the slow axis parallel to the retarder plane and perpendicular to a thickness direction of the retarder sheet. The fixed +A type retarders 714 have a same retardation magnitude of 130nm but different azimuthal angles of -8.4°, -3.8°, -42.7°, and 0.2°.

[0085] The required retardation magnitude and orientation angles have been obtained by running a computer-based optimization routine with the aim of having the PCS 704 match the circular-to-linear polarization transformation by the first 711 and/or second 712 MTN LC cells in the undriven or low-voltage state, i.e. a transformation similar to the one illustrated in FIG. 1 above. The goal of the optimization is to make sure that the PCS 704 converts the input polarization state of the plurality of spectral components of the impinging light 702 to the mid-way polarization states wavelength-dispersed along a line of intersection of a Poincaré sphere with a mid-way plane between the first and second polarization states on the Poincaré sphere, as explained above with reference to FIG. 4. For the case of the LHCP and RHCP output polarizations, the mid-way plane is the plane of the equator circle of the Poincaré sphere where linear polarizations of different orientations are located.

[0086] The locations of the linear polarizations for different spectral components of the impinging light 702 may be extracted by inputting light at an achromatic circular polarization to the first 711 and/or second 712 LC cell in the undriven state, and measuring the wavelength distribution of orientations of the quasi-linear polarization exiting the first 711 and/or second 712 LC cells. The measured profile is specific to the LC cell configuration, including twist angle, cell gap, and birefringence dispersion. The PCS 704 configuration thus has an engineered dispersion that optimizes performance, subject to a balance between the output polarization states.

[0087] The $\theta(\lambda)$ target profile may be extracted from the specific MTN cell configuration. The incremental ellipticity may be ignored in some embodiments, with the goal of producing a linear SOP with the target angle profile at all wavelengths of interest. A series of search and global minimization routines was used to extract the stack configuration illustrated in FIGs. 7A and 7B. The stack uses five fixed +A type retarders 714, which are layers of uniaxial quarter-wave 130nm retarder film with the orientation of the slow axis for each layer tabulated at the bottom of each retarder 714 in FIGs. 7A and 7B. In practice, these films can be laminated using pressure-sensitive-adhesives (PSAs), or solvent-laminated. The polarization transformation paths of the PCS 704 are illustrated in FIG. 5.

[0088] The first 711 and second 712 LC cells have a same thickness-direction retardation R_{th} in the driven state. The compensator plate 715 may be configured to at least partially compensate the R_{th} of one of the first 711 or second 712 LC cells in the driven state. To that end, the R_{th} compensator plate 715 may include e.g. a –C fixed retarder, specifically –C retarder with the retardation of 145nm. Herein and throughout the rest of the specification, the term "–C retarder" means a uniaxial retarder having an extraordinary refractive index smaller than the ordinary refractive index, with the slow axis parallel to the thickness direction of the retarder sheet and perpendicular to the plane of the retarder sheet.

[0089] A polarization transformation path of the light 702 propagating through the polarization switch 700 in the state of FIG. 7A, i.e. when the first LC cell 711 is not energized and the second LC cell 712 is energized, is illustrated in FIG. 8A. The input SOP of the light 702 is a linear polarization indicated as "Linear Input" at the equator 122 of the Poincaré sphere

120 in FIG. 8A. The normal-incidence output polarization state is left-hand circular polarization state indicated as "LHCP Output" at the bottom of the Poincaré sphere 120 in FIG. 8A. The polarization transformation paths for red (R), green (G), and blue (B) components of the light beam 702 are indicated in FIG. 8 with dashed, solid, and dashed-dotted curved lines respectively.

[0090] The PCS 704 delivers the optimum, wavelength-dispersed linear SOP of the light 702 at the red, green, and blue wavelengths to the first LC cell 711. The first LC cell 711 then transforms the wavelength-dispersed linear polarization to LHCP. The overall transformation is substantially achromatic because, as noted above, the PCS 704 has been constructed to match the wavelength dispersion of the polarization transformation by the first LC cell 711 in the low-voltage or undriven state. Furthermore, the combination of the passive -C plate with adjacent fully energized second LC Cell 2 minimizes the composite R_{th}, maximizing the contrast at non-normal angles of incidence of the light 702.

[0091] A polarization transformation path of the light 702 propagating through the polarization switch 700 in the state of FIG. 7B, i.e. when the first LC cell 711 is energized and the second LC cell 712 is not energized, is illustrated in FIG. 8B. The input SOP of the light 702 (FIGs. 7A and 7B) is a linear polarization indicated as "Linear Input" at the equator 122 of the Poincaré sphere 120 of FIG. 8B. The normal-incidence output polarization state is right-hand circular polarization state indicated as "RHCP Output" at the top of the Poincaré sphere 120 in FIG. 8B. Similarly to FIG. 8A, the PCS 704 delivers the optimum linear SOP of the light 702 at the red, green, and blue wavelengths to the first LC cell 711, which substantially does not change the polarization distribution. The light beam 702 then propagates through the compensator plate 715 and impinges onto the second LC cell 712. The second LC cell 712 transforms the wavelength-dispersed linear polarization to RHCP. The overall transformation is substantially achromatic, because the PCS 704 has been constructed to match the wavelength dispersion of the polarization transformation by the second LC cell 712 in the low-voltage or undriven state. Each one of the first 711 and second 712 LC cells is compensated, because the first 711 and second 712 cells are substantially identical if not for the direction of the director twist. The combination of the passive -C plate with adjacent fully energized second LC Cell 2 minimizes the composite R_{th}, maximizing the contrast at non-normal angles of incidence of the light 702.

Example 2: Linear-to-Circular Switch Using Biaxial PCS and MTN LC Cells

[0092] Turning to FIGs. 9A and 9B, a polarization switch 900 is an embodiment of the polarization switch 700 of FIGs. 7A and 7B, includes same or similar elements, and operates by a similar principle. The polarization switch 900 of FIGs. 9A and 9B converts the linear polarization state of the light 702 defined by the input polarizer 705 into one of mutually orthogonal LHCP and RHCP states, which may be substantially achromatic over an entire spectral width of visible light.

[0093] The polarization switch 900 of FIGs. 9A and 9B includes a PCS 904, the first 711 and second 712 MTN LC cells of the polarization switch 700, and the compensator plate 715 of the polarization switch 700 between the first 711 and second 712 MTN LC cells. The PCS 904 includes a stack of fixed retarders 914, which are 130nm QW retarders that satisfy the condition $n_z = (n_x + n_y)/2$. Such retarders are denoted as "0R_{th} 130" in FIGs. 9A and 9B. The stack angles shown in FIGs. 9A and 9B correspond to the polarization transformations illustrated in FIG. 6. As in Example 1, the first 711 and second 712 LC are driven anti-phase, with the combined action of the PCS 904 and the first LC cell 711 producing LHCP, and the combined action of the PCS 904 with the second LC cell 712 producing RHCP. The retardation magnitude and orientation angles have been obtained by running a computer-based optimization with the aim of having the PCS 904 match the circular-to-linear polarization transformation by the first 711 and/or second 712 LC cells in the undriven or low-voltage state.

[0094] Rays were traced through the polarization switch 900 in each output state, covering a normal angle of incidence (AOI) to a 30° AOI range, versus azimuth. For each ray angle, the output SOP was determined at each wavelength. This was then projected onto ideal circular analyzers, which gives the transmission and leakage. The ratio of the former to the latter gives the contrast. This contrast is given by

[0095] $$Contrast = \left(\frac{1+\bar{\varepsilon}}{1-\bar{\varepsilon}}\right)^2 \quad (6)$$

[0096] where $\bar{\varepsilon}$ is the ellipticity field ratio. The transmission and leakage values were determined over the entire 400nm – 700nm band, which were then converted to a photopic contrast number. This is shown in the contrast polar plots of FIGs. 10A and 10B. The contrast at normal incidence is >2,000:1 and exceeds 1,000:1 over much of the angle range. At the worst-case azimuth in each state, the photopic contrast at 30° AOI is approximately 200:1.

Example 3: Circular Polarization Handedness Switching Using MTN LC Cells

[0097] Polarization optical elements with true circular eigen-polarizations have optical performance dependent on handedness of impinging circularly polarized light. Twisted photo-patterned reactive-mesogen (RM) coatings can be used to make diffractive optical elements for e.g. focusing or steering light. By stacking RM layers, these elements can have high diffraction efficiency over a broad range of wavelengths. Such elements may require polarization switches that act on circular polarization, giving binary switching between functional eigen-polarizations. Switches paired with Pancharatnam Berry Phase (PBP) lenses, for example, can give binary focal length adjustment as needed for accommodation in AR/VR headsets.

[0098] Referring now to FIGs. 11A and 11B, a polarization switch 1100 is an embodiment of the 700 of FIGs. 7A and 7B, includes same or similar elements, and operates by a similar principle. The polarization switch 1100 of FIGs. 11A and 11B converts LHCP polarization state of impinging light 1102 into one of mutually orthogonal LHCP and RHCP states, which may be substantially achromatic over an entire spectral width of visible light. FIG. 11A corresponds to LHCP to LHCP transformation, i.e. the case when the LHCP polarization is preserved over the spectral range of interest, while FIG. 11B corresponds to the LHCP to RHCP transformation, i.e. the case when the handedness of the input circular polarization is flipped.

[0099] The polarization switch 1100 of FIGs. 11A and 11B includes a PCS 1104 coupled to the first 711 and second 712 MTN LC cells with the compensator plate 715 in between as in the polarization switch 700 of FIGs. 7A and 7B. The PCS 1104 includes a stack of the fixed $0R_{th}$ retarders 914 of FIGs. 9A and 9B, but at different azimuthal angles. In the PCS 1104 of FIGs. 11A and 11B, the angles are -87.9°; 26.2°; 6.8°; 8.5°; and 77.0°.

[00100] The polarization switch 1100 is an actively compensated switch that either leaves an incident circular polarization unchanged (State 1; FIG. 11A), or it converts the input to the orthogonal circular SOP (State 2; FIG 11B). The former requires a zero composite R_e (i.e. functionally isotropic), and the latter requires a half-wave of composite $R_e(=\lambda/2)$. In this example, the PCS 1104 maps the SOP from an achromatic circular state to the previous wavelength dispersed linear polarization, $\theta(\lambda)$. FIG. 12 shows a polarization transformation path by the PCS 1104, with (1), (2), (3), (4), and (5) indicating transformation by corresponding first, second, third, fourth, and fifth $0R_{th}$ fixed retarders 914, respectively, along a propagation path of the light 1102 in the stack of the PCS 1104. The polarization transformation paths of the red, green, and blue light are shown in FIG. 12 with dashed, solid, and dashed-dotted lines, respectively.

[00101] With the second LC cell 712 driven to the +C plate state, an isotropic state requires that the first LC cell in combination with the PCS produce zero composite R_e. The path is from the north-pole to the equator, and back to the north pole ("LHCP INPUT/OUTPUT in FIG. 12). As a general requirement, this is equivalent to stating that the circular input SOP is an eigen-polarization of the combined first LC cell and PCS. This includes the degenerate case where combined the first LC cell with the PCS is functionally isotropic (i.e. the composite Jones matrix is the identity matrix). This would be the case if the PCS 1104 were instead a passive copy of the cell, but with a reverse-order-crossed director field. This disclosure encompasses PCS configurations like this, comprising one or more passive layers of twisted LC material. With that the first LC cell driven to the +C plate state, the second LC cell in combination with the PCS must provide an achromatic half-wave of retardation. That is, the PCS 1104 optimally disperses the SOP along the equator according to $\theta(\lambda)$, such that the second LC cell maps that input to the orthogonal pole.

[00102] FIGs. 13A and 13B are photopic contrast polar plots for the configuration of FIGs. 11A and 11B respectively, where the isotropic state corresponds to the top of Poincaré sphere in FIG. 12, and the half-wave state corresponds to the bottom of Poincaré sphere in FIG. 12. The contrast at normal incidence is >2,000:1 and again exceeds 1,000:1 over much of the angle

range. At the worst-case azimuth in each state, the photopic contrast at 30° AOI is approximately 220:1 for the isotropic state and 168:1 for the half-wave state.

[00103] Table 2 below summarizes the performance of the PCS, as well as the RGB ellipticity, of the two output states of the polarization switch 700 of FIGs. 7A and 7B (Example 1), the polarization switch 900 of FIGs. 9A and 9B (Example 2), and the polarization switch 1100 of FIGs. 11A and 11B (Example 3).

Table 2. Summary of ellipticity and orientation for MTN, PCS, and switch examples. MTN x1, one LC cell; MTN x2, a pair of LC cells; Ex 1, 2, 3, Examples 1, 2, 3 respectively.

Device	$\theta(650nm)$	$\bar{\varepsilon}(650nm)$	$\theta(550nm)$	$\bar{\varepsilon}(550nm)$	$\theta(450nm)$	$\bar{\varepsilon}(450nm)$
MTN x1	21.0°	0.038	13.6°	0.034	0.2°	0.008
Ex1 PCS	19.1°	0.004	14.6°	0.009	-0.2°	0.024
Ex2 PCS	21.1°	0.002	14.3°	0.002	0.8°	0.002
Ex3 PCS	21.0°	0.007	13.9°	0.002	0.4°	0.007
MTN x2	-	0.854	-	0.865	-	0.927
Ex1 State 1	-	0.910	-	0.939	-	0.935
Ex1 State 2	-	0.897	-	0.913	-	0.966
Ex2 State 1	-	0.918	-	0.920	-	0.945
Ex2 State 2	-	0.930	-	0.936	-	0.977
Ex3 State 1	-	0.884	-	0.945	-	0.979
Ex3 State 2	-	0.939	-	0.956	-	0.965

[00104] A general approach to constructing a polarization switch, consistent with the above examples, may be exemplified by a method 1400 including:

- Determining (1402) the pair of orthogonal SOPs that a polarization switch must switch between, as well as the spectral range of interest;
- Locating (1404) a Poincaré mirror plane mid-way between these orthogonal SOPs, as explained above with reference to FIG. 4;
- Identifying (FIG. 14; 1406) an LC cell configuration that transforms either of the desired outputs to lie on the Poincaré mirror plane over the spectral range of interest. Optimally,

the LC device maps all spectral components to the mirror plane, with an arbitrary distribution;

- Determining (1408) the distribution of polarization states versus wavelength on the Poincaré mirror plane, by simulation or direct measurement;
- Identifying (1410) the input polarization constraints, e.g. an achromatic input. If there is flexibility in the input (e.g. orientation), use that as a design degree of freedom;
- For the specific LC cell configuration, providing (1412) a PCS that maps the (achromatic) input to the distribution of polarization states versus wavelength;
- Arranging (1414) a pair of matched LC cells, such that LC cell 1 in combination with the PCS maps the input SOP to a first output SOP, and LC cell 2 in combination with the PCS maps the input SOP to a second output SOP.

[00105] Referring now to FIG. 15, a method 1500 for configuring a polarization switch to convert an input polarization state of light into one of mutually orthogonal first or second polarization states includes configuring (1502) a PCS to convert the input polarization state to a mid-way polarization state wavelength-dispersed along a line of intersection of a Poincaré sphere with a mid-way plane between the first and second polarization states on the Poincaré sphere. First and second LC cells may be configured (1504) to convert the mid-way polarization state into the first and second polarization states, respectively, when in an undriven state. The PCS configuring 1502 may include determining (1506) a wavelength dispersion of a polarization transformation by the at least one of the first or second LC cells in the undriven state within the spectral bandwidth, and offsetting the wavelength dispersion of polarization transformation by at least one of the first or second LC cells within the spectral bandwidth. More specifically, the PCS configuring may include selecting (1508) retardation values and azimuthal orientations of each fixed retarder of a stack of fixed retarders, e.g. by running a global optimization routine to offset the wavelength-selective polarization transformations by the (MTN) LC cell(s).

[00106] Switches of this disclosure are of particular use in applications that require a high degree of isolation between orthogonal states when using broadband (e.g. 400nm to 700nm) light

over a wide range of incidence angles. This is particularly so when errors in retardation translate into cross-talk leakages that determine the contrast ratio of an optical system. For example, Pancharatnam-Berry Phase (PBP) lenses and gratings are passive diffractive lenses with circular eigen-polarizations, each corresponding to a particular sign of a focal length / diffraction direction. By switching the handedness of input polarization precisely, the focal length of output light can likewise be switched precisely.

[00107] Examples of PBP lenses and gratings having optical performance switchable by utilizing a polarization switch of this disclosure will now be presented. Referring to FIG. 16A, an Pancharatnam–Berry phase (PBP) LC lens 1600 includes LC molecules 1602 in an LC layer 1604. The LC molecules 1602 are disposed in XY plane at a varying in-plane orientation depending on the distance r from the lens center. The orientation angle $\phi(r)$ of the LC molecules 1602 in the liquid crystal layer 1604 of the PBP LC lens 1600 is given by

[00108] $$\phi(r) = \frac{\pi r^2}{2 f_o \lambda_o} \qquad (7a)$$

[00109] where f_o is a desired focal length and λ_o is wavelength. The optical phase delay in the PBP LC lens 1600 is due to Pancharatnam–Berry phase, or geometrical phase effect. An optical retardation R of the liquid crystal layer 1604 having a thickness t is defined as $R = t\Delta n$, where Δn is the optical birefringence of the LC layer 1604. At the optical retardation R of the LC layer 1604 of $\lambda_o/2$, i.e. half wavelength, the accumulated phase delay $P(r)$ due to the PBP effect can be expressed rather simply as $P(r) = 2\phi(r)$, or, by taking into account Eq. (7a) above,

[00110] $$P(r) = \frac{\pi r^2}{f_o \lambda_o} \qquad (7b)$$

[00111] It is the quadratic dependence of the PBP $P(r)$ on the radial coordinate r that results in the focusing, or defocusing, function of the LC PBP lens 1600. This is different from a conventional LC spatial phase modulator (SLM), which utilizes changes in the tilt angle to provide a spatial phase distribution, and often has a discontinuity at a boundary of 2π modulo. A

PBP device, such as the PBP lens 1600, has the azimuthal angle ϕ continuously and smoothly varying across the surface of the LC layer 1604 as illustrated in FIG. 16B. Accordingly, the mapping of the azimuthal angle to PBP, i.e. $P(r) = 2\phi(r)$ when $R = \lambda_o/2$, allows for a more drastic phase change without introducing discontinuities at a boundary of 2π modulo typically present in a conventional LC SLM.

[00112] The optical performance of the PBP LC lens 1600 is illustrated in FIG. 17. In FIG. 17, the LC molecules of the PBP LC lens 1600 are disposed predominantly in-plane, i.e. in XY plane. The optical retardation of the PBP LC lens 1600 is a half wavelength; thus, the PBP LC lens 1600 acts as a half-wave waveplate with spatially varying fast axis, changing the polarization of incoming light from LHCP to RHCP, and vice versa. A sign, or direction, of the phase profile of a PBP device depends on polarization of an impinging light beam 1700. By way of example, when the impinging light beam 1700 is LHCP, the phase delay at the lens center decreases toward the periphery of the PBP LC lens 1600, such that the PBP LC lens 1600 focuses the beam 1700, which becomes RHCP. The focused RHCP beam 1700 is shown with solid lines. When an incoming light beam 1700 is RHCP, the phase delay at the lens center increases toward the periphery of the PBP LC lens 1600, such that the PBP LC lens 1600 defocuses the beam 1700, which becomes LH circularly polarized. The defocused LHCP beam 1700 is shown with dashed lines.

[00113] Turning to FIGs. 18A and 18B, a PBP LC grating 1800 includes LC molecules 1802 in an LC layer 1804. The LC molecules 1802 are disposed in XY plane at a varying in-plane orientation depending on the X coordinate. The orientation angle $\phi(x)$ of the LC molecules 1802 in the PBP LC grating 1800 is given by

[00114] $$\phi(x) = \pi x/\mathrm{T} = \pi x \sin\theta / \lambda_o \qquad (8)$$

[00115] where θ is a diffraction angle given by

[00116] $$\theta = \sin^{-1}(\lambda_o / \mathrm{T}) \qquad (9)$$

[00117] where T is pitch of the PBP LC grating 1800. The azimuthal angle ϕ varies continuously across the surface of the LC layer 1804 as illustrated in FIG. 18B, with the constant pitch T. By comparison, the pitch T of the azimuthal angle ϕ variation in FIG. 16B is not constant, i.e. T_1 is generally not equal to T_2. The optical phase delay P in the PBP LC grating 1800 of FIG. 18A is also due to the PBP effect, i.e. $P(r) = 2\phi(x)$ when $R = \lambda_o/2$.

[00118] Optical performance of the PBP LC grating 1800 is illustrated in FIG. 19. The LC molecules 1802 are disposed predominantly in-plane, i.e. in XY plane. When an impinging light beam 1900 is LH circularly polarized, the PBP LC grating 1800 redirects the light beam 1900 upwards, which becomes RH circularly polarized. The RCP deflected light beam 1900 is shown with solid lines. When the impinging light beam 1900 is RH circularly polarized, the PBP LC grating 1800 redirects the light beam 1900 downwards, which becomes LH circularly polarized. The LH circularly polarized deflected light beam 1900 is shown with dashed lines.

[00119] Stacks of N switches/PBP lenses can create digital accommodation switching with up to 2^N distinct focal lengths and/or diffraction directions. Errors in polarization in switching correspond to power being projected along the unwanted PBP eigen-polarization. This translates directly to cross-talk and image degradation. Polarization switches of this disclosure enable a high degree of isolation between states.

[00120] Referring to FIG. 20, an augmented reality (AR) near-eye display (NED) 2000 may use polarization switches disclosed herein to switch and/or expand field of view, to provide variable focusing, etc. The VR NED 2000 includes a frame 2001 supporting, for each eye: an image projector 2002 for providing image light carrying an image to be displayed; a pupil-replicating lightguide 2004 for guiding the image light inside and out-coupling portions of the image light towards an eyebox 2012; a refocusing lens 2006 for refocusing the image light to provide virtual images at an adjustable virtual image plane; a focus correction lens 2008 for undoing the refocusing by the refocusing lens 2006 for outside light; an eye-tracking camera 2010; and a plurality of eyebox illuminators 2014 shown as black dots. The refocusing lens 2006 and/or the focus correction lens 2008 may include polarization switch(es) and PBP lens(es) disclosed herein.

[00121] The purpose of the eye-tracking cameras 2010 is to determine position and/or orientation of both eyes of the user to enable steering the output image light to the locations of the user's eyes. The illuminators 2014 illuminate the eyes at the corresponding eyeboxes 2012, to enable the eye-tracking cameras 2010 to obtain the images of the eyes, as well as to provide reference reflections i.e. glints. The glints may function as reference points in the captured eye image, facilitating the eye gazing direction determination by determining position of the eye pupil images relative to the glints images. To avoid distracting the user with the light of the eyebox illuminators 2014, the light illuminating the eyeboxes 2012 may be made invisible to the user. For example, infrared light may be used to illuminate the eyeboxes 2012.

[00122] Turning to FIG. 21, an HMD 2100 is an example of an AR/VR wearable display system which encloses the user's face, for a greater degree of immersion into the AR/VR environment. The HMD 2100 may generate the entirely virtual 3D imagery. The HMD 2100 may include a front body 2102 and a band 2104 that can be secured around the user's head. The front body 2102 is configured for placement in front of eyes of a user in a reliable and comfortable manner. A display system 2180 may be disposed in the front body 2102 for presenting AR/VR imagery to the user. The display system 2180 may include any of the polarization switches disclosed herein. Sides 2106 of the front body 2102 may be opaque or transparent.

[00123] In some embodiments, the front body 2102 includes locators 2108 and an inertial measurement unit (IMU) 2110 for tracking acceleration of the HMD 2100, and position sensors 2112 for tracking position of the HMD 2100. The IMU 2110 is an electronic device that generates data indicating a position of the HMD 2100 based on measurement signals received from one or more of position sensors 2112, which generate one or more measurement signals in response to motion of the HMD 2100. Examples of position sensors 2112 include: one or more accelerometers, one or more gyroscopes, one or more magnetometers, another suitable type of sensor that detects motion, a type of sensor used for error correction of the IMU 2110, or some combination thereof. The position sensors 2112 may be located external to the IMU 2110, internal to the IMU 2110, or some combination thereof.

[00124] The locators 2108 are traced by an external imaging device of a virtual reality system, such that the virtual reality system can track the location and orientation of the entire HMD 2100. Information generated by the IMU 2110 and the position sensors 2112 may be compared with the position and orientation obtained by tracking the locators 2108, for improved tracking accuracy of position and orientation of the HMD 2100. Accurate position and orientation is important for presenting appropriate virtual scenery to the user as the latter moves and turns in 3D space.

[00125] The HMD 2100 may further include a depth camera assembly (DCA) 2111, which captures data describing depth information of a local area surrounding some or all of the HMD 2100. The depth information may be compared with the information from the IMU 2110, for better accuracy of determination of position and orientation of the HMD 2100 in 3D space.

[00126] The HMD 2100 may further include an eye tracking system 2114 for determining orientation and position of user's eyes in real time. The obtained position and orientation of the eyes also allows the HMD 2100 to determine the gaze direction of the user and to adjust the image generated by the display system 2180 accordingly. The determined gaze direction and vergence angle may be used to adjust the display system 2180 to reduce the vergence-accommodation conflict. The direction and vergence may also be used for displays' exit pupil steering as disclosed herein. Furthermore, the determined vergence and gaze angles may be used for interaction with the user, highlighting objects, bringing objects to the foreground, creating additional objects or pointers, etc. An audio system may also be provided including e.g. a set of small speakers built into the front body 2102.

[00127] Embodiments of the present disclosure may include, or be implemented in conjunction with, an artificial reality system. An artificial reality system adjusts sensory information about outside world obtained through the senses such as visual information, audio, touch (somatosensation) information, acceleration, balance, etc., in some manner before presentation to a user. By way of non-limiting examples, artificial reality may include virtual reality (VR), augmented reality (AR), mixed reality (MR), hybrid reality, or some combination and/or derivatives thereof. Artificial reality content may include entirely generated content or generated content combined with captured (e.g., real-world) content. The artificial reality

content may include video, audio, somatic or haptic feedback, or some combination thereof. Any of this content may be presented in a single channel or in multiple channels, such as in a stereo video that produces a three-dimensional effect to the viewer. Furthermore, in some embodiments, artificial reality may also be associated with applications, products, accessories, services, or some combination thereof, that are used to, for example, create content in artificial reality and/or are otherwise used in (e.g., perform activities in) artificial reality. The artificial reality system that provides the artificial reality content may be implemented on various platforms, including a wearable display such as an HMD connected to a host computer system, a standalone HMD, a near-eye display having a form factor of eyeglasses, a mobile device or computing system, or any other hardware platform capable of providing artificial reality content to one or more viewers.

[00128] The present disclosure is not to be limited in scope by the specific embodiments described herein. Indeed, other various embodiments and modifications, in addition to those described herein, will be apparent to those of ordinary skill in the art from the foregoing description and accompanying drawings. Thus, such other embodiments and modifications are intended to fall within the scope of the present disclosure. Further, although the present disclosure has been described herein in the context of a particular implementation in a particular environment for a particular purpose, those of ordinary skill in the art will recognize that its usefulness is not limited thereto and that the present disclosure may be beneficially implemented in any number of environments for any number of purposes. Accordingly, the claims set forth below should be construed in view of the full breadth and spirit of the present disclosure as described herein.

WHAT IS CLAIMED IS:

1. A polarization switch for converting an input polarization state of light into one of mutually orthogonal first or second polarization states, the polarization switch comprising:

first and second liquid crystal (LC) cells each comprising a non-zero in-plane retardation in an undriven state; and

a passive compensation structure (PCS) configured to convert the input polarization state to the first polarization state together with the first LC cell in the undriven state, and to convert the input polarization state to the second polarization state together with the second LC cell in the undriven state;

wherein:

the light has a plurality of spectral components; and

the PCS is configured to convert the input polarization state of the plurality of spectral components to mid-way polarization states wavelength-dispersed along a line of intersection of a Poincaré sphere with a mid-way plane between the first and second polarization states on the Poincaré sphere.

2. The polarization switch of claim 1, wherein the first and second LC cells each comprise a twisted nematic (TN) LC cell.

3. The polarization switch of claim 2, wherein the first and second TN LC cells have substantially same functional parameters other than a twist direction.

4. The polarization switch of claim 1, wherein the first and second LC cells have a substantially zero in-plane retardation in a driven state.

5. The polarization switch of claim 1, wherein:

the spectral components of the light in the first polarization state are within 15 degrees from one another on the Poincaré sphere; and

the spectral components of the light in the second polarization state are within 15 degrees from one another on the Poincaré sphere.

6. The polarization switch of claim 1, wherein the PCS is configured to offset a wavelength dispersion of the in-plane retardation of either one of the first and second LC cells in the undriven state within a spectral bandwidth of the plurality of spectral components.

7. The polarization switch of claim 1, wherein the PCS comprises a stack of fixed retarders.

8. The polarization switch of claim 7, wherein the fixed retarders comprise +A retarders oriented at different azimuthal angles for converting the input polarization state of the plurality of spectral components to the wavelength-dispersed mid-way polarization states.

9. The polarization switch of claim 1, wherein the first and second LC cells have a same thickness-direction retardation R_{th} in a driven state, the polarization switch further comprising an R_{th} compensator for compensating the thickness-direction retardation R_{th} of one of the first or second LC cells in the driven state.

10. The polarization switch of claim 9, wherein the R_{th} compensator is disposed between the first and second LC cells.

11. The polarization switch of claim 10, wherein the R_{th} compensator comprises a –C fixed retarder.

12. The polarization switch of claim 1, further comprising a controller operably coupled to the first and second LC cells and configured to perform at least one of:

drive the second LC cell to a driven state while having the first LC cell in the undriven state to convert the input polarization state to the first polarization state; or

drive the first LC cell to a driven state while having the second LC cell in the undriven state to convert the input polarization state to the second polarization state.

13. The polarization switch of claim 12, wherein:

driving the second or first LC cell to the driven state comprises applying a first voltage to the first or second LC cell respectively; and

having the first or second LC cell in the undriven state comprises applying a second voltage to the first or second LC cell respectively;

wherein the second voltage is lower than the first voltage.

14. A method for configuring a polarization switch to convert an input polarization state of light into one of mutually orthogonal first or second polarization states, the method comprising:

configuring a passive compensation structure (PCS) to convert the input polarization state to a mid-way polarization state wavelength-dispersed along a line of intersection of a Poincaré sphere with a mid-way plane between the first and second polarization states on the Poincaré sphere; and

configuring first and second liquid crystal (LC) cells to convert the mid-way polarization state into the first and second polarization states, respectively, when in an undriven state.

15. The method of claim 14, wherein the light has a plurality of spectral components within a spectral bandwidth, wherein the PCS is configured to offset a wavelength dispersion of polarization transformation by at least one of the first or second LC cells in an undriven state within the spectral bandwidth.

16. The method of claim 15, further comprising determining the wavelength dispersion of the polarization transformation by the at least one of the first or second LC cells in the undriven state within the spectral bandwidth.

17. The method of claim 14, wherein the PCS comprises a stack of fixed retarders, and wherein configuring the PCS comprises selecting retardation values and azimuthal orientations of the fixed retarders of the stack.

18. A passive compensation structure (PCS) for a twisted nematic (TN) LC cell configured to convert an input polarization state of light impinging onto the TN LC cell into a first polarization state wavelength-dispersed along a mid-way plane between the input polarization state and an output substantially achromatic polarization state orthogonal to the input polarization state;

the PCS comprising a stack of fixed retarders configured to convert the input polarization state of light impinging onto the PCS into a second wavelength-dispersed polarization state matching the first wavelength-dispersed polarization state.

19. The PCS of claim 18, wherein a twist angle of the TN LC cell is less than 90 degrees.

20. The PCS of claim 18, wherein the fixed retarders comprise +A retarders oriented at different azimuthal angles.

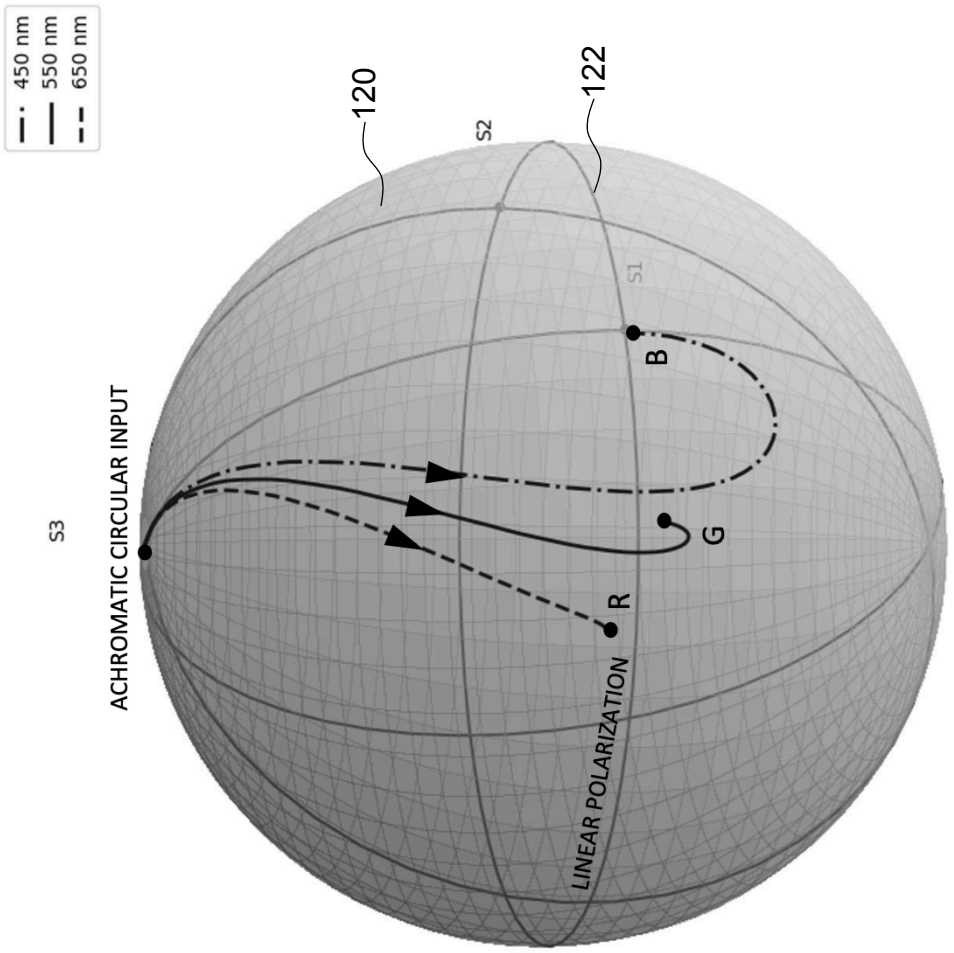
450 nm
550 nm
650 nm
120
122
S2
S1
S3
ACHROMATIC CIRCULAR INPUT
B
G
R
LINEAR POLARIZATION

FIG. 1

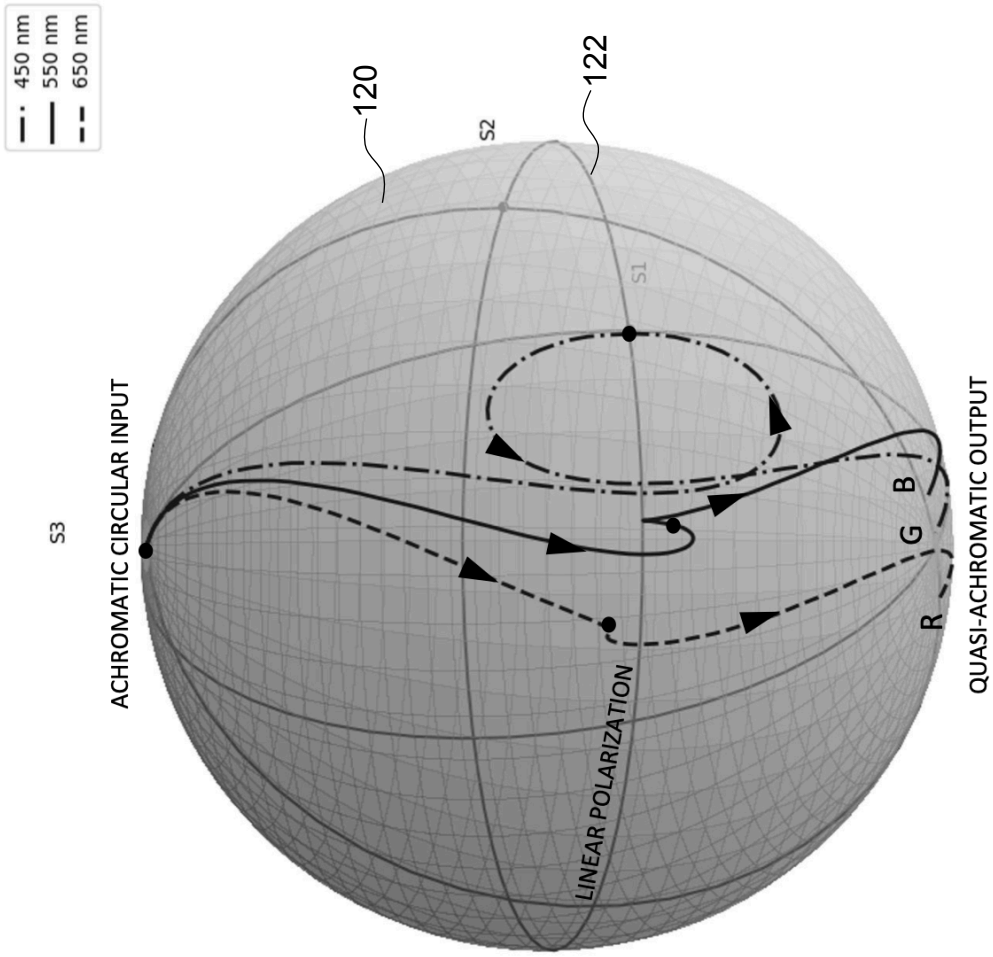
450 nm
550 nm
650 nm
120
122
S1
S2
S3
ACHROMATIC CIRCULAR INPUT
QUASI-ACHROMATIC OUTPUT
LINEAR POLARIZATION
R
G
B

FIG. 2

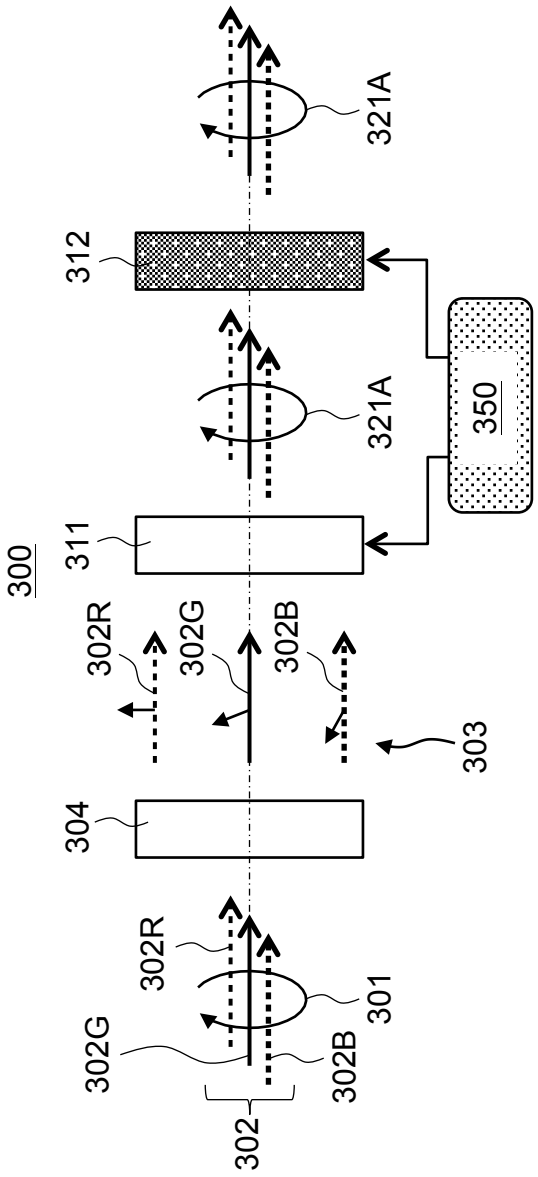
300
302R
302G
302B
303
304
311
312
321A
321A
350
302R
302G
302B
301
302

FIG. 3A

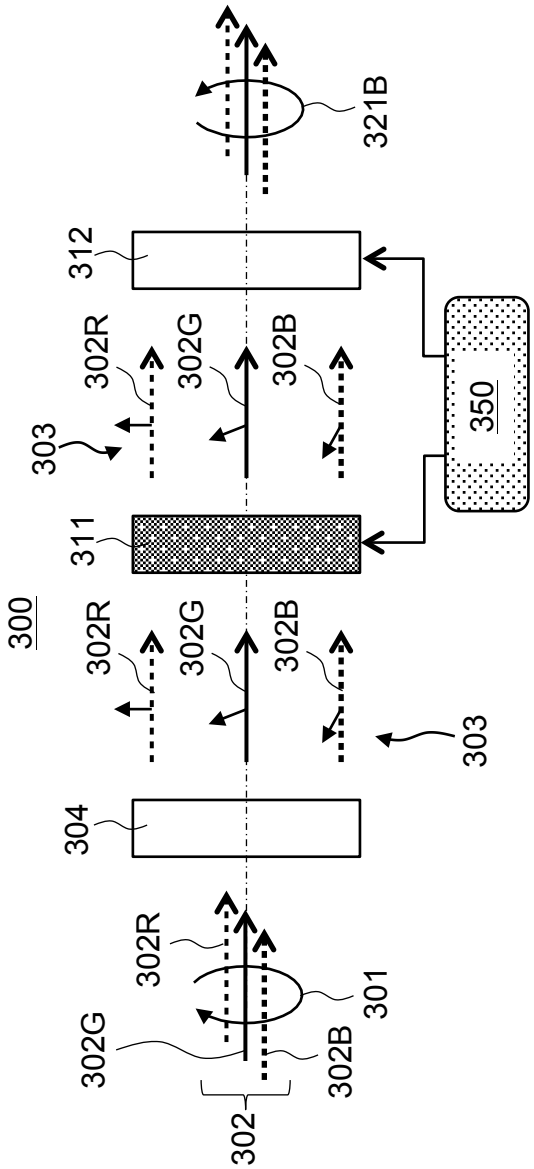
300
302R
302G
302B
303
304
311
312
321B
350
302R
302G
302B
301
302

FIG. 3B

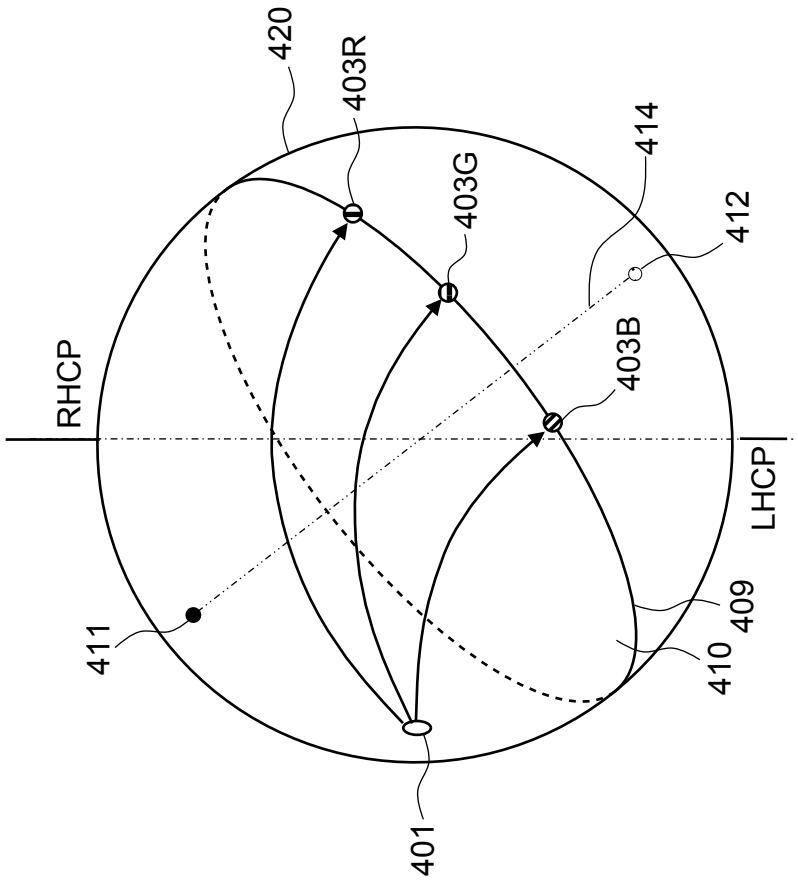

FIG. 4

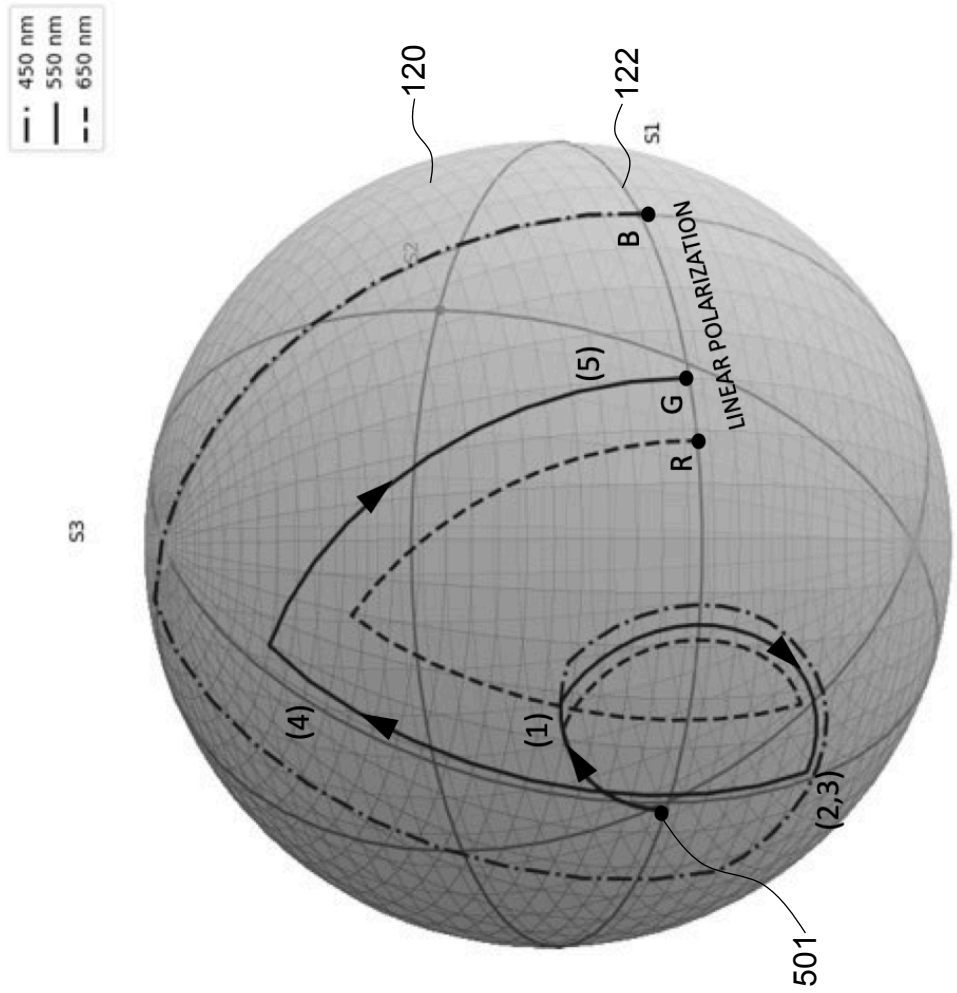
450 nm
550 nm
650 nm
120
122
S1
S2
S3
B
G
R
LINEAR POLARIZATION
(1)
(2,3)
(4)
(5)
501

FIG. 5

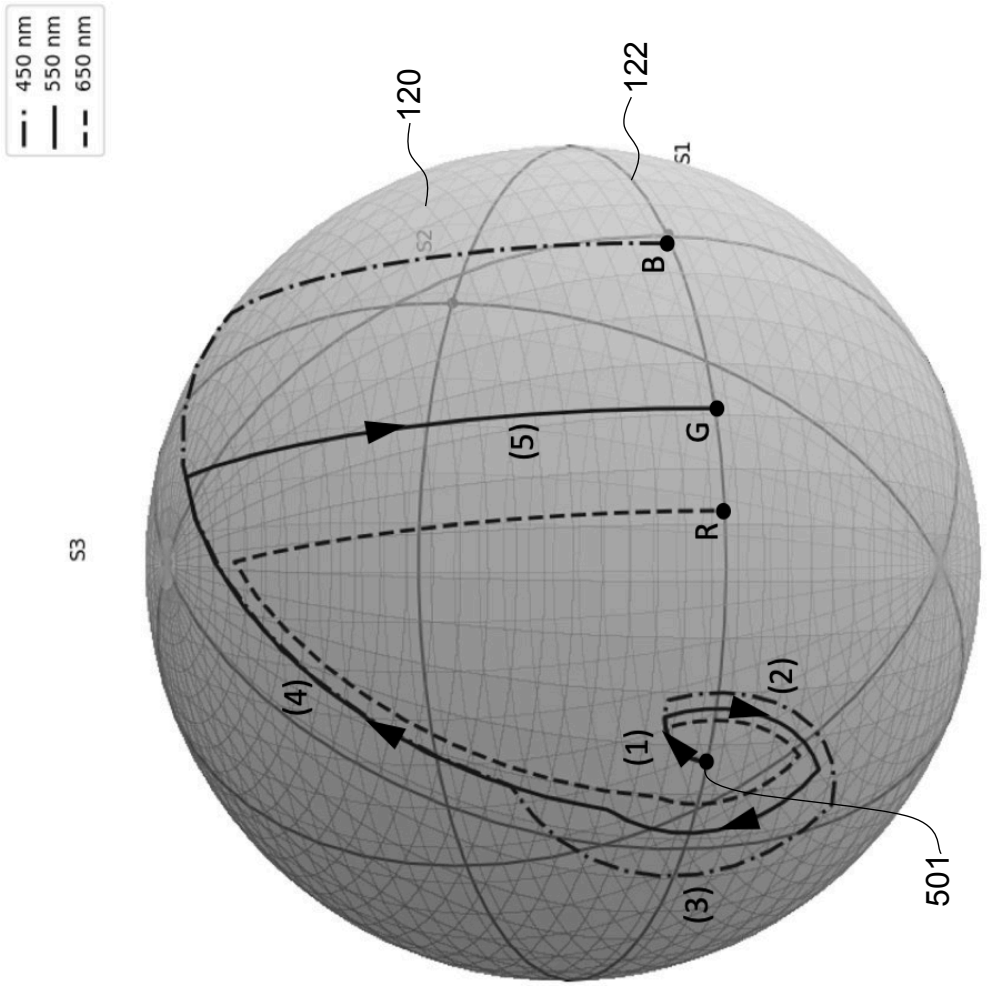

FIG. 6

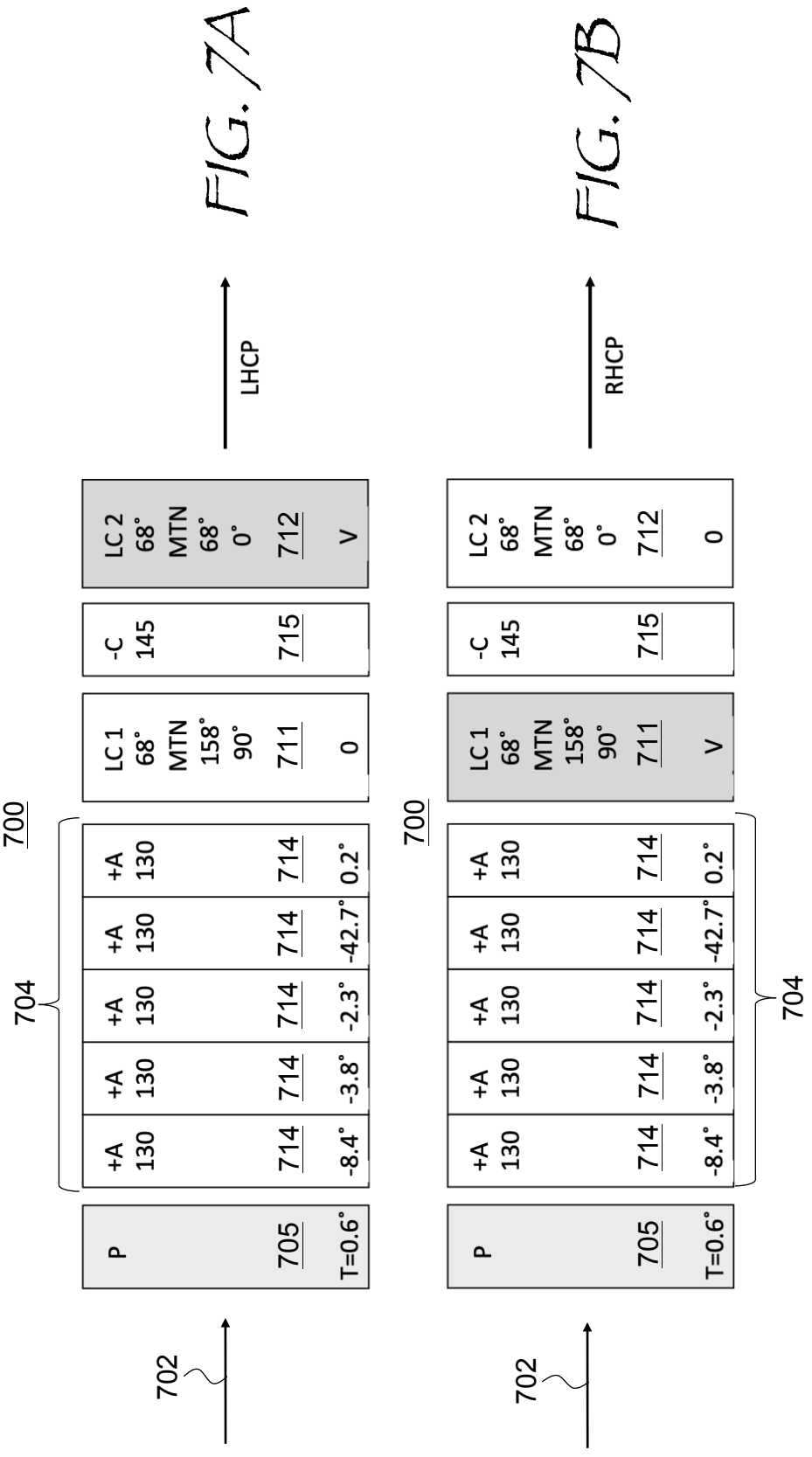
700
704
702
P
+A 130
705
T=0.6°
714
-8.4°
-3.8°
-2.3°
-42.7°
0.2°
LC 1 68° MTN 158° 90°
711
0
-C 145
715
LC 2 68° MTN 68° 0°
712
V
LHCP
RHCP

FIG. 7A

FIG. 7B

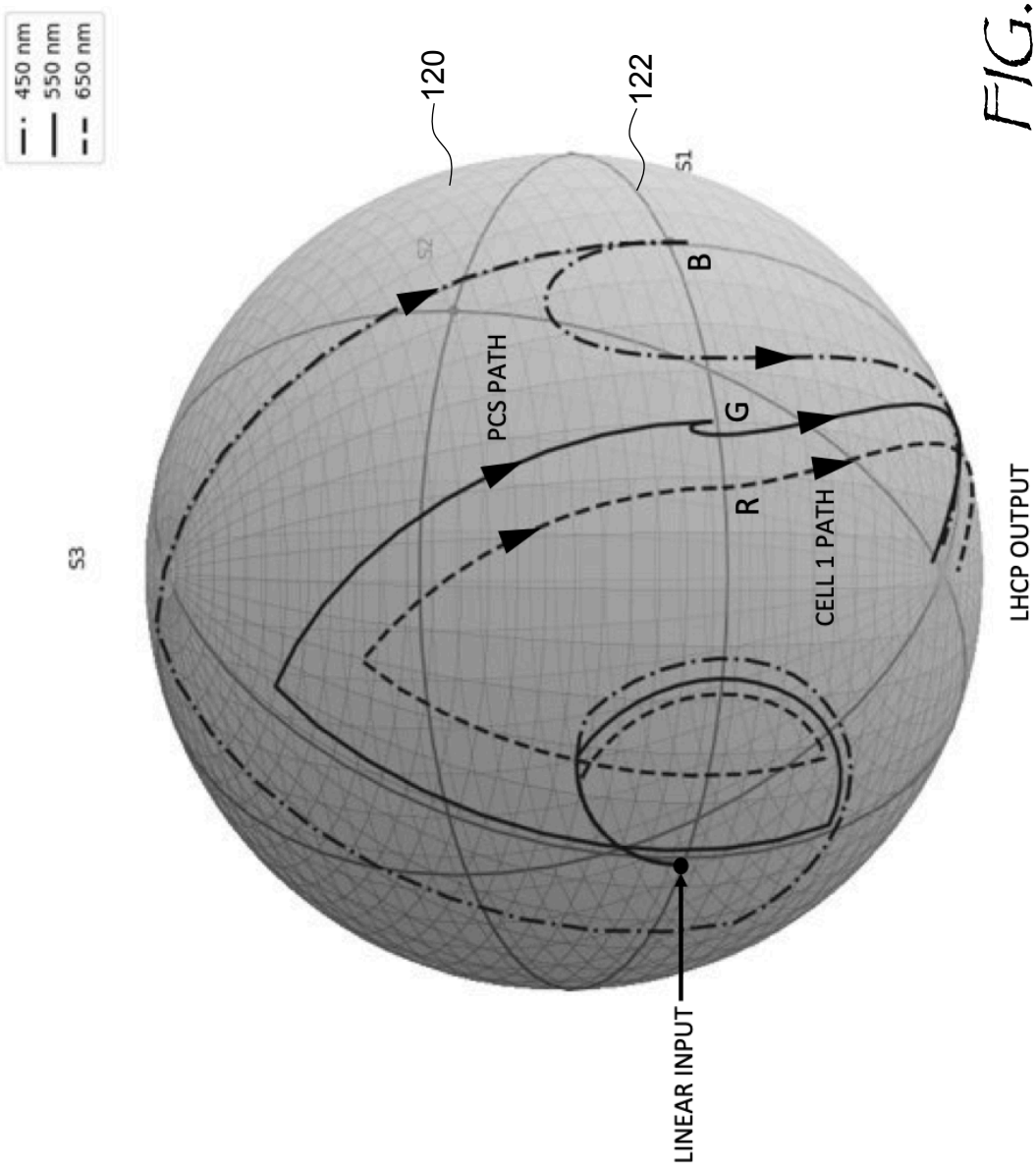
450 nm
550 nm
650 nm
120
122
S1
S2
S3
B
G
R
PCS PATH
CELL 1 PATH
LINEAR INPUT
LHCP OUTPUT

FIG. 8A

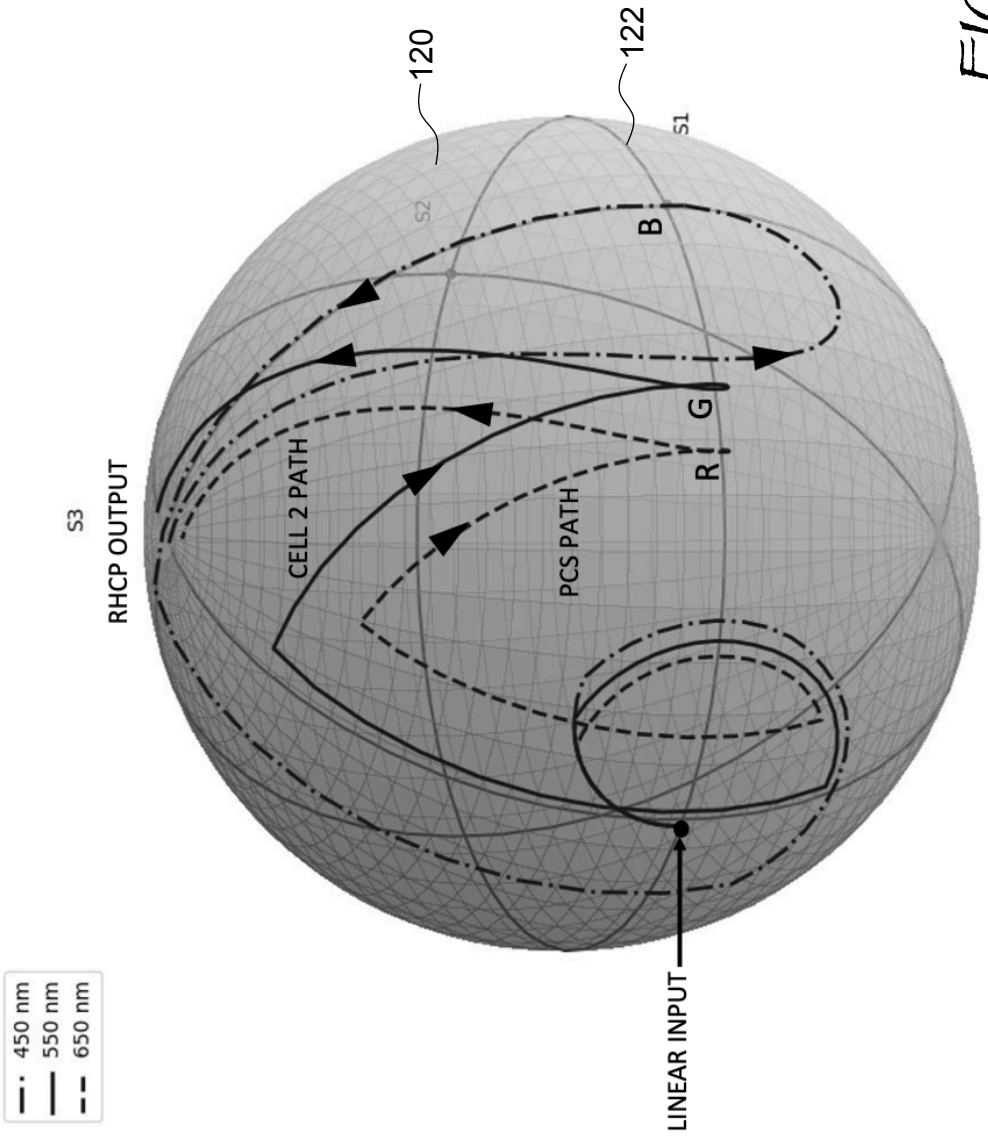
120
122
S1
S2
S3
B
G
R
CELL 2 PATH
PCS PATH
RHCP OUTPUT
LINEAR INPUT
450 nm
550 nm
650 nm

FIG. 8B

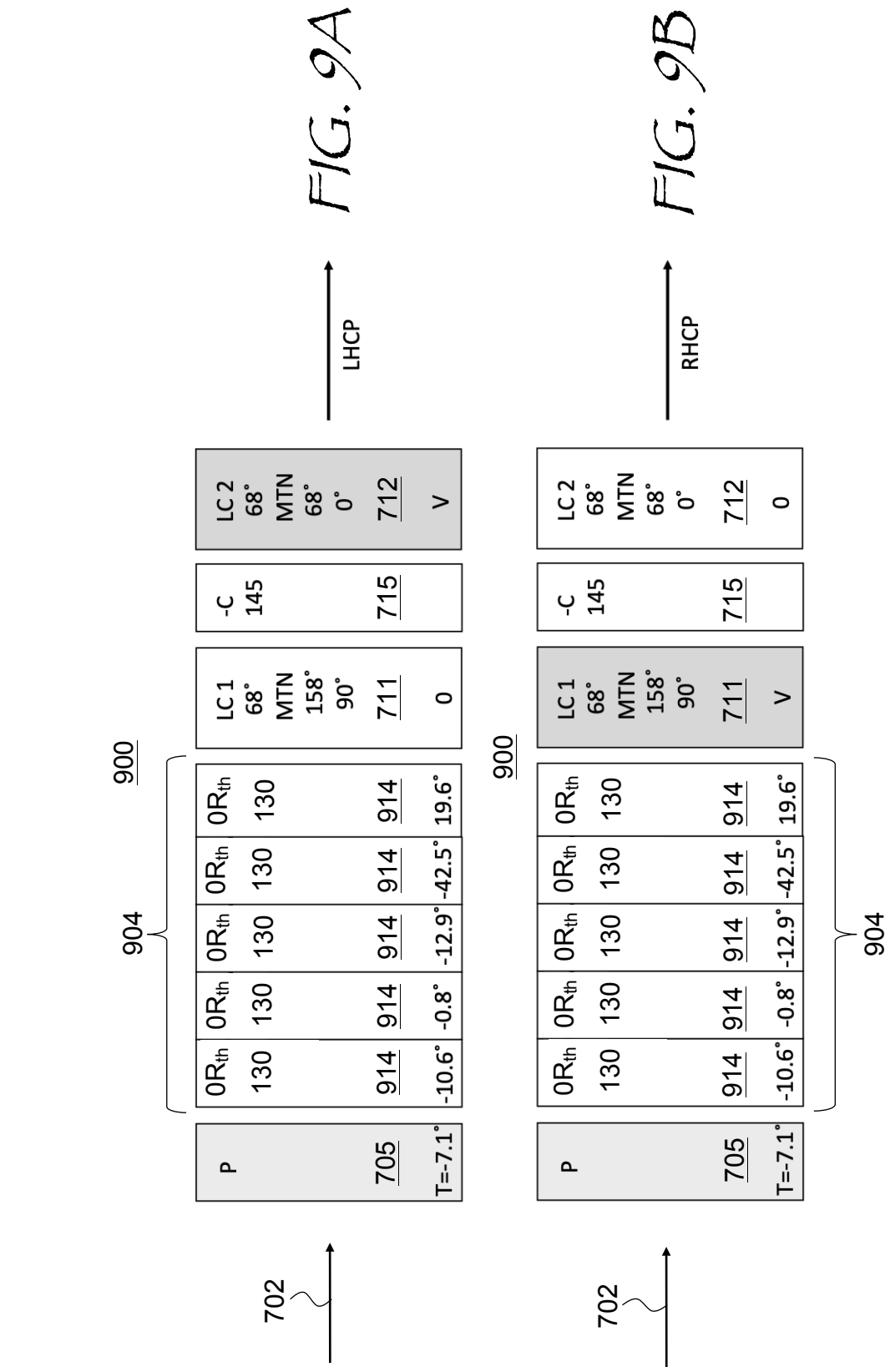
900
904
P
705
T=-7.1°
0R_th
130
914
-10.6°
0R_th
130
914
-0.8°
0R_th
130
914
-12.9°
0R_th
130
914
-42.5°
0R_th
130
914
19.6°
LC 1
68°
MTN
158°
90°
711
0
-C
145
715
LC 2
68°
MTN
68°
0°
712
V
LHCP
702
900
904
P
705
T=-7.1°
0R_th
130
914
-10.6°
0R_th
130
914
-0.8°
0R_th
130
914
-12.9°
0R_th
130
914
-42.5°
0R_th
130
914
19.6°
LC 1
68°
MTN
158°
90°
711
V
-C
145
715
LC 2
68°
MTN
68°
0°
712
0
RHCP
702

FIG. 9A

FIG. 9B

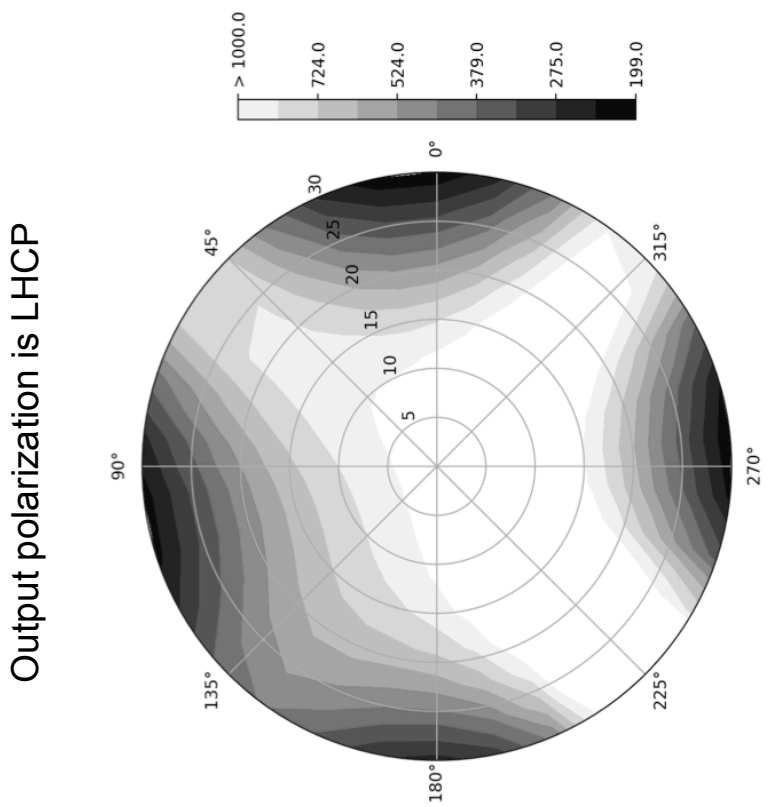

FIG. 10A

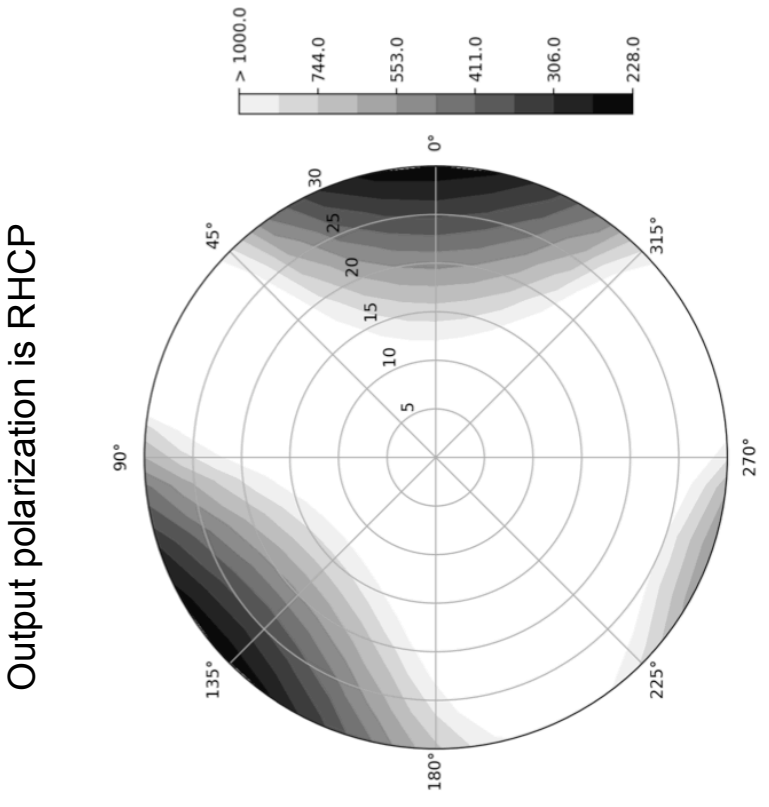

FIG. 10B

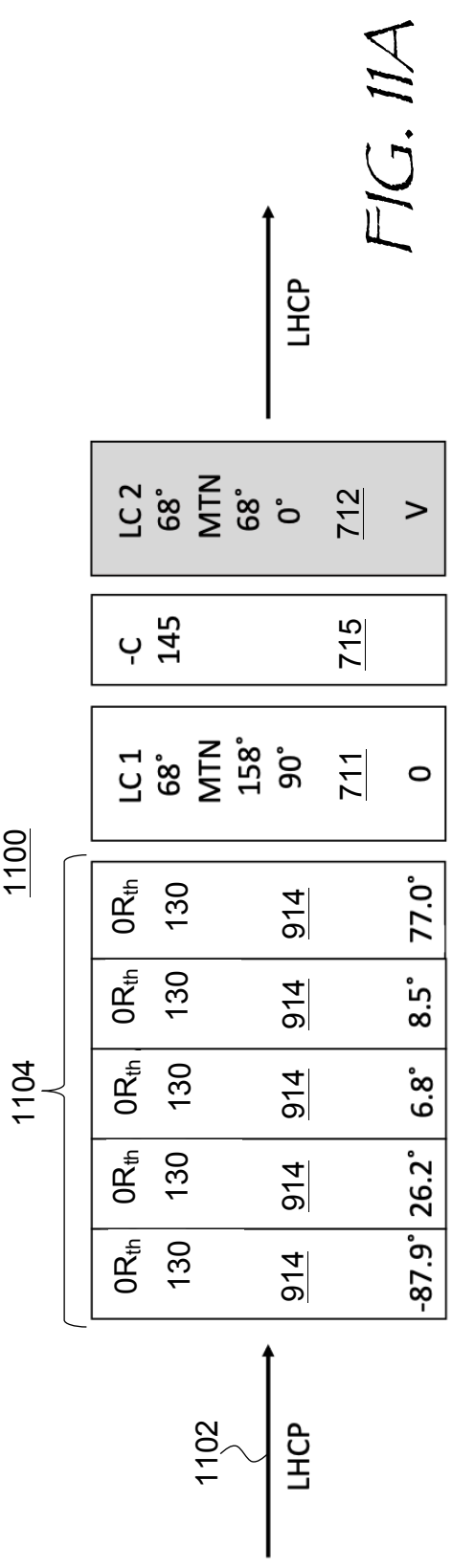

FIG. 11A

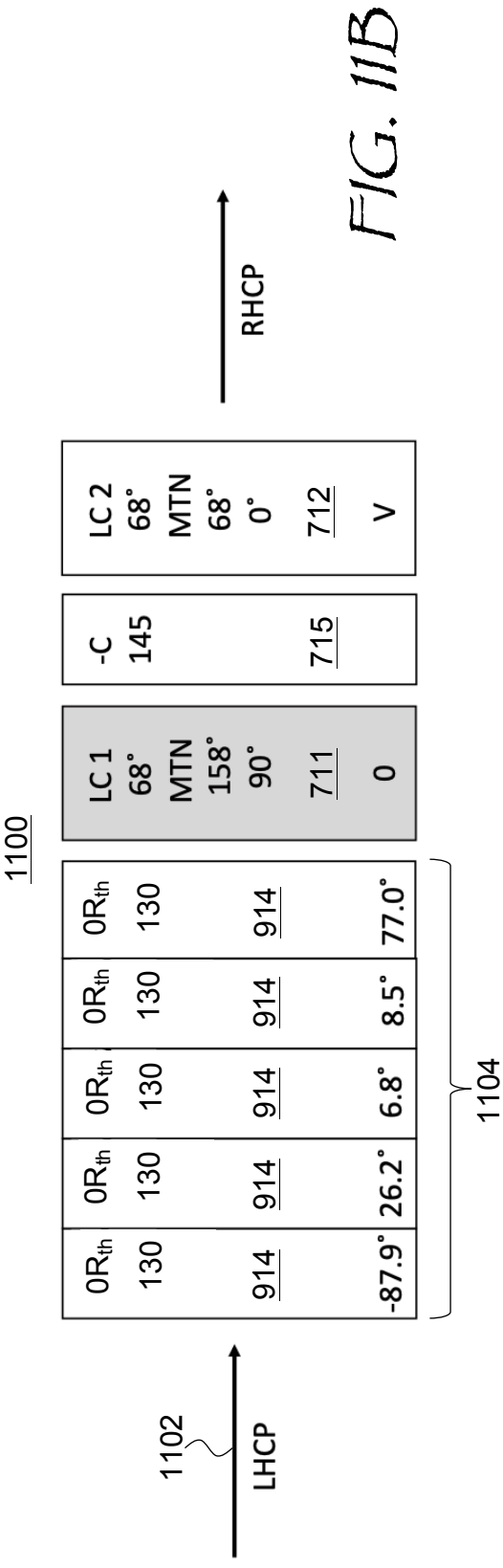

FIG. 11B

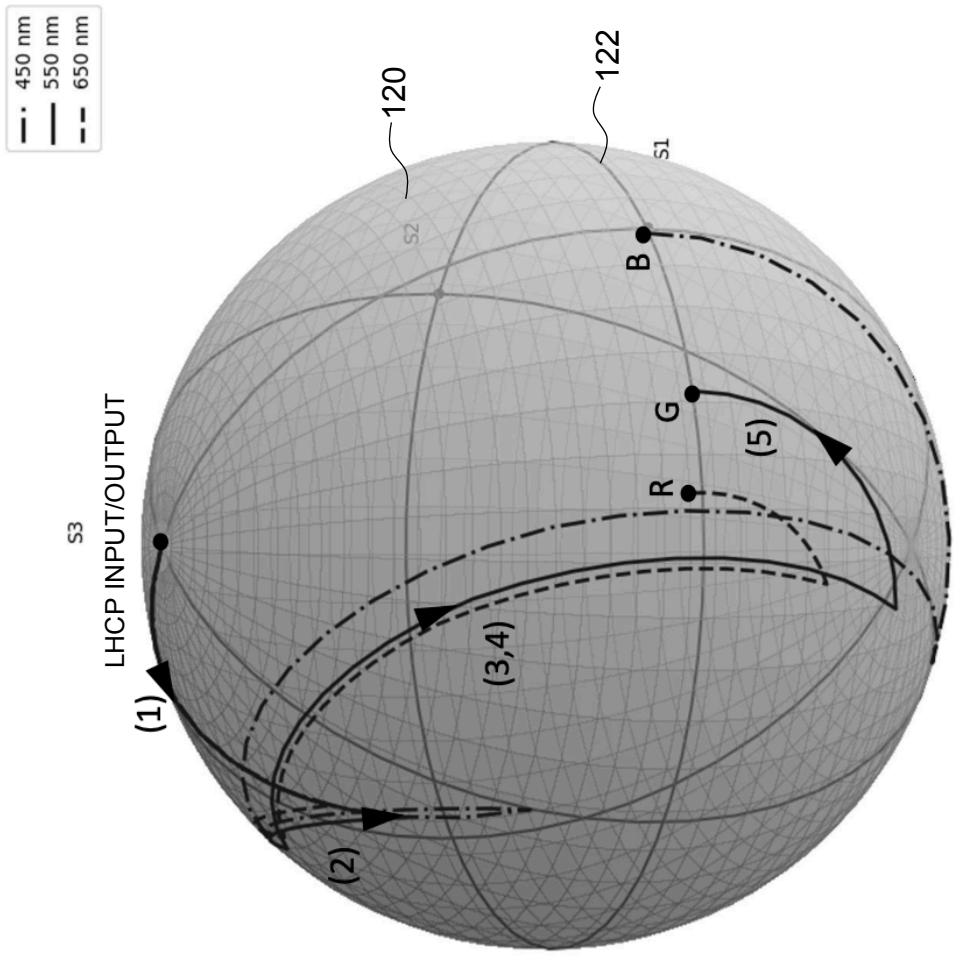
450 nm
550 nm
650 nm
120
122
S1
S2
S3
B
G
R
(1)
(2)
(3,4)
(5)
LHCP INPUT/OUTPUT
RHCP OUTPUT

FIG. 12

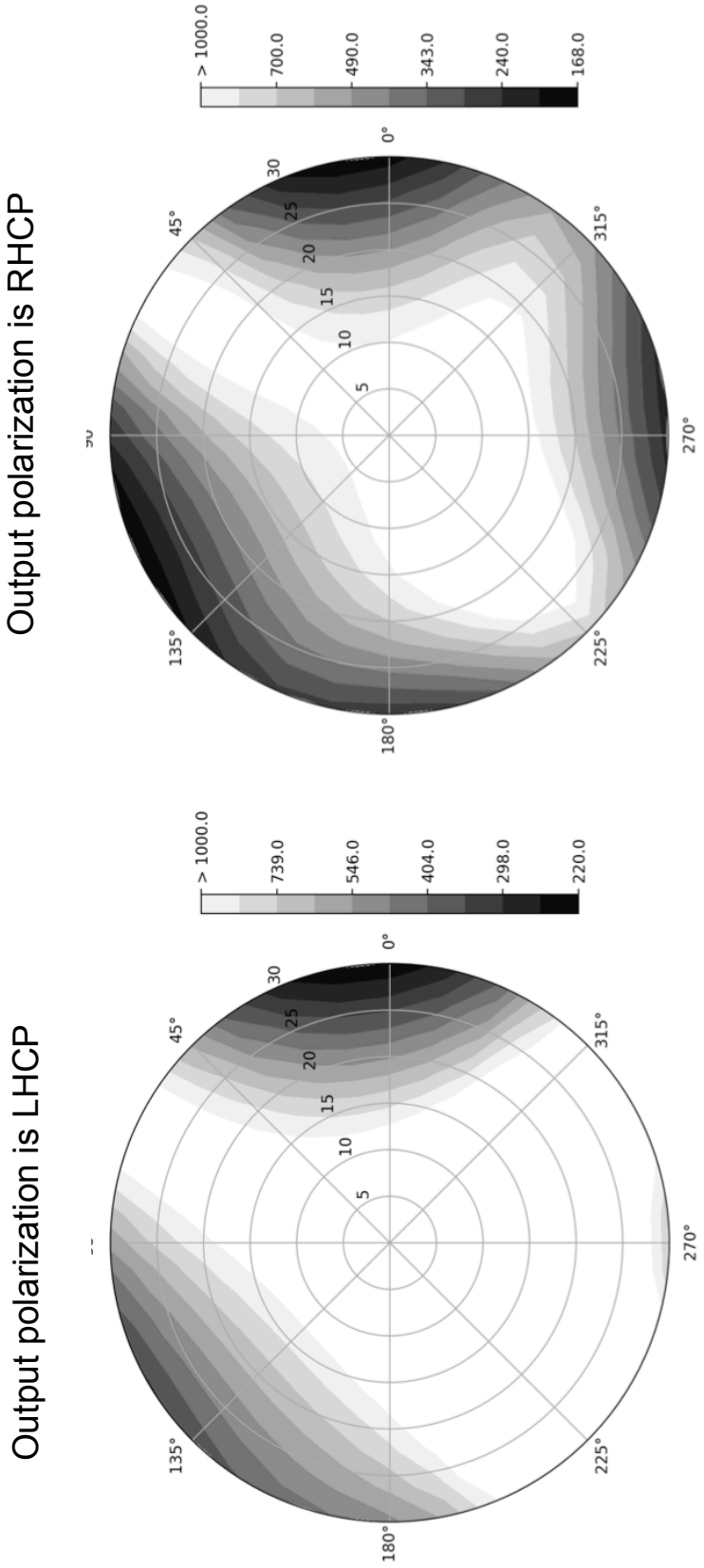

FIG. 13A

FIG. 13B

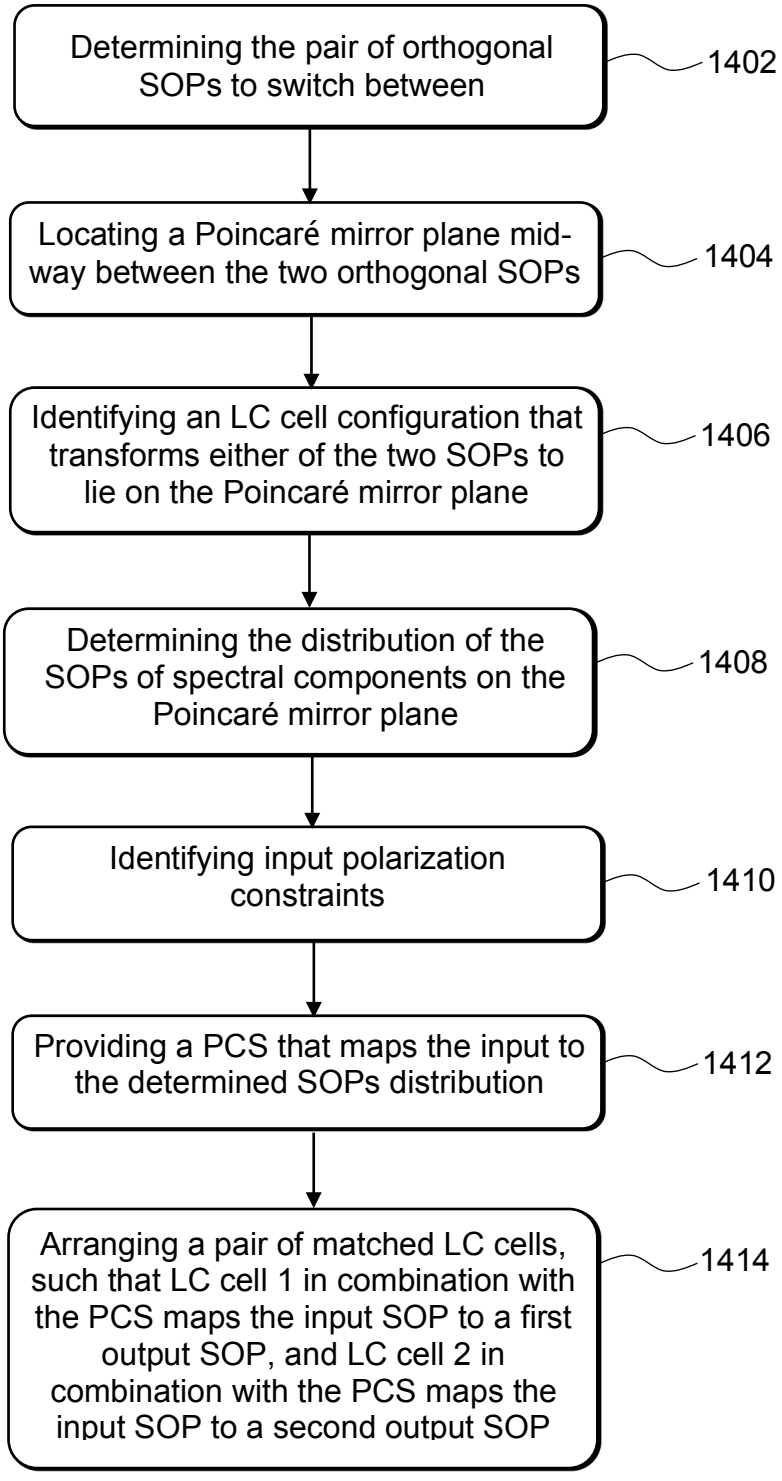
Determining the pair of orthogonal SOPs to switch between
1402
Locating a Poincaré mirror plane mid-way between the two orthogonal SOPs
1404
1400
Identifying an LC cell configuration that transforms either of the two SOPs to lie on the Poincaré mirror plane
1406
Determining the distribution of the SOPs of spectral components on the Poincaré mirror plane
1408
Identifying input polarization constraints
1410
Providing a PCS that maps the input to the determined SOPs distribution
1412
Arranging a pair of matched LC cells, such that LC cell 1 in combination with the PCS maps the input SOP to a first output SOP, and LC cell 2 in combination with the PCS maps the input SOP to a second output SOP
1414

FIG. 14

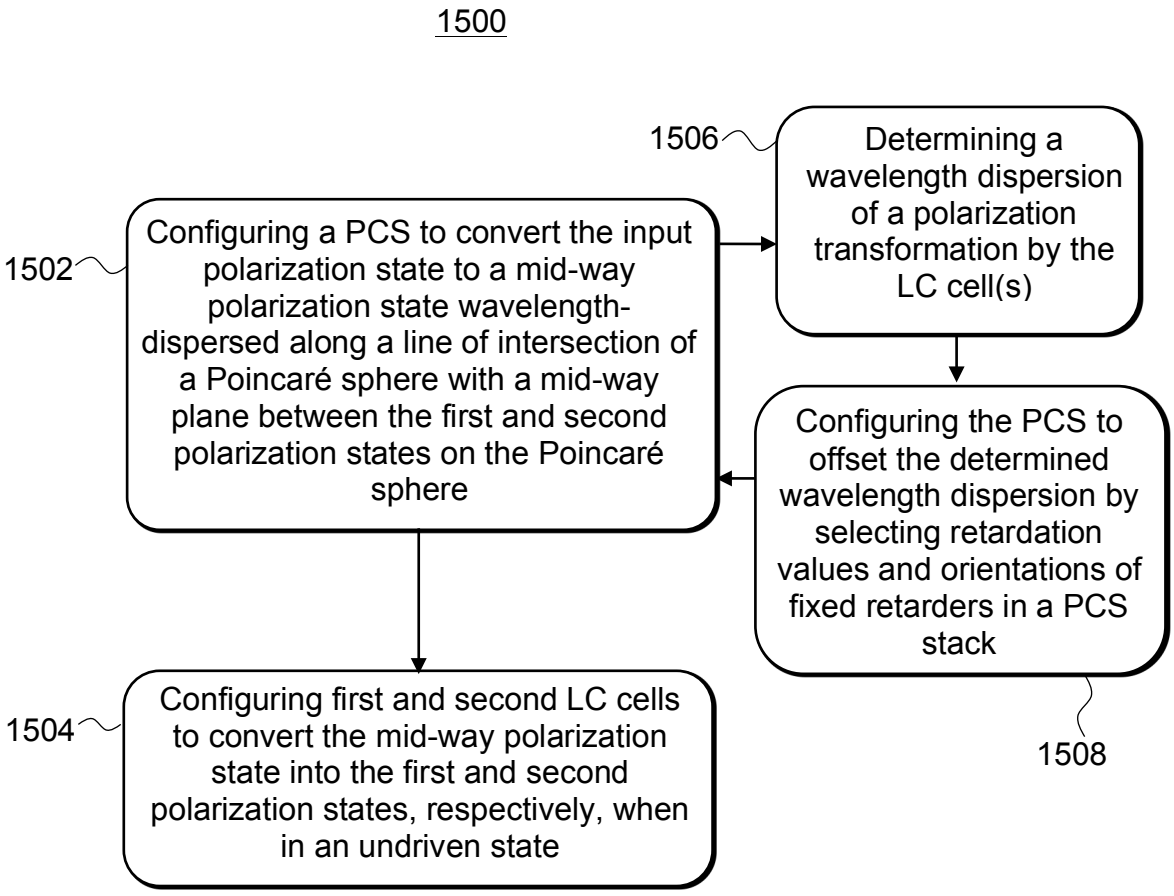
1500
1506
Determining a wavelength dispersion of a polarization transformation by the LC cell(s)
1502
Configuring a PCS to convert the input polarization state to a mid-way polarization state wavelength-dispersed along a line of intersection of a Poincaré sphere with a mid-way plane between the first and second polarization states on the Poincaré sphere
Configuring the PCS to offset the determined wavelength dispersion by selecting retardation values and orientations of fixed retarders in a PCS stack
1508
1504
Configuring first and second LC cells to convert the mid-way polarization state into the first and second polarization states, respectively, when in an undriven state

FIG. 15

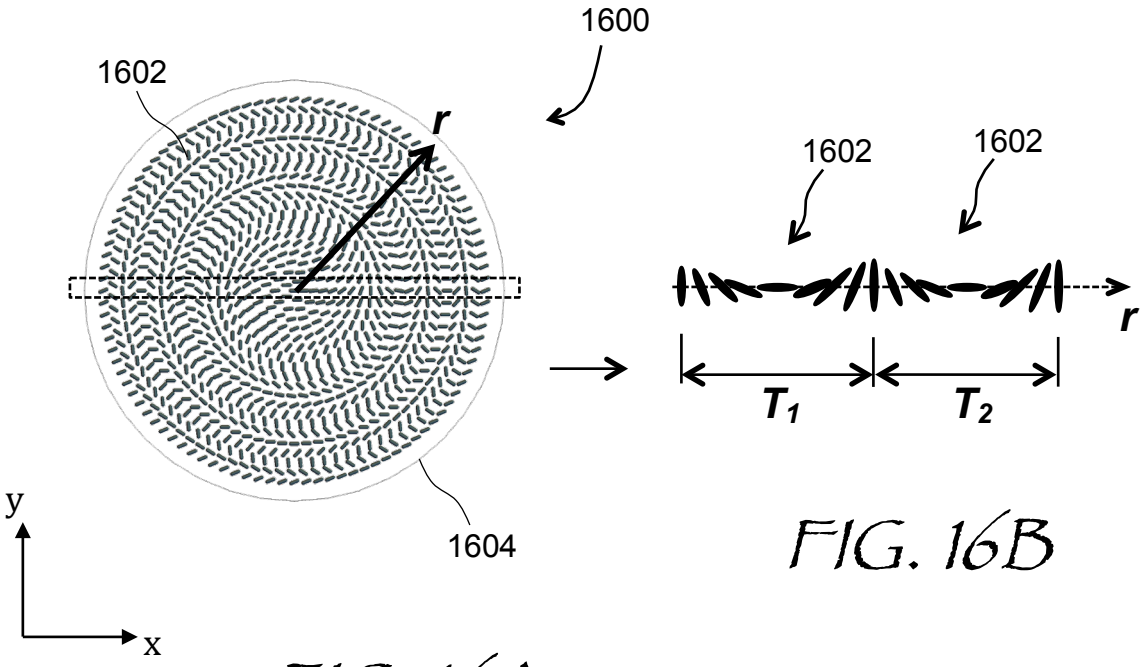

FIG. 16A

FIG. 16B

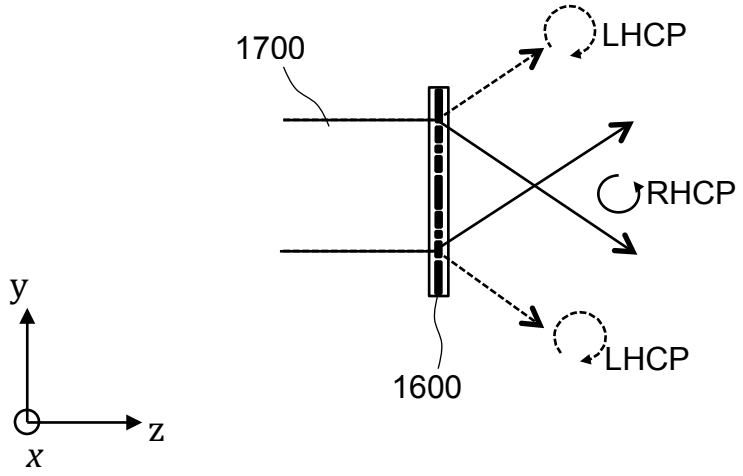

FIG. 17

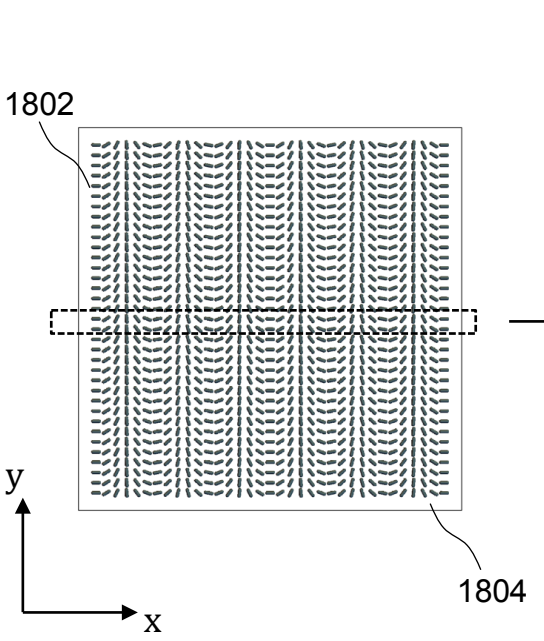

FIG. 18A

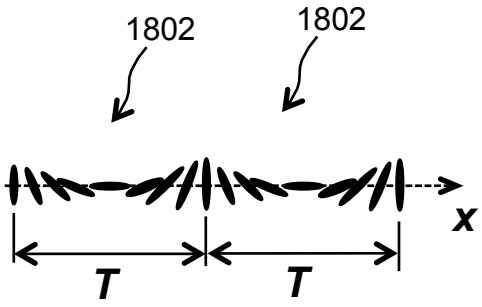

FIG. 18B

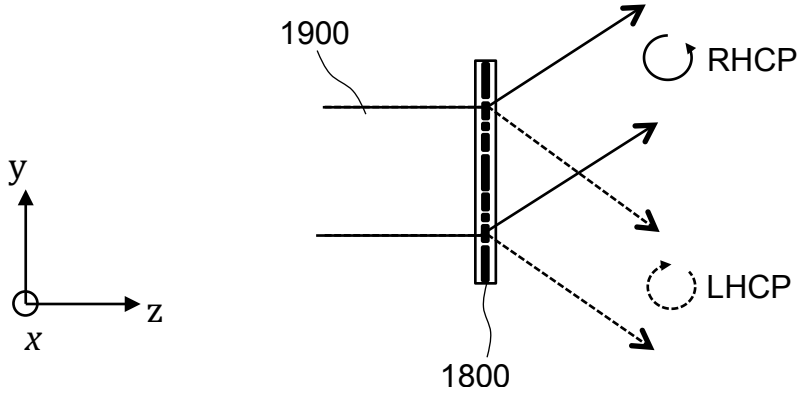

FIG. 19

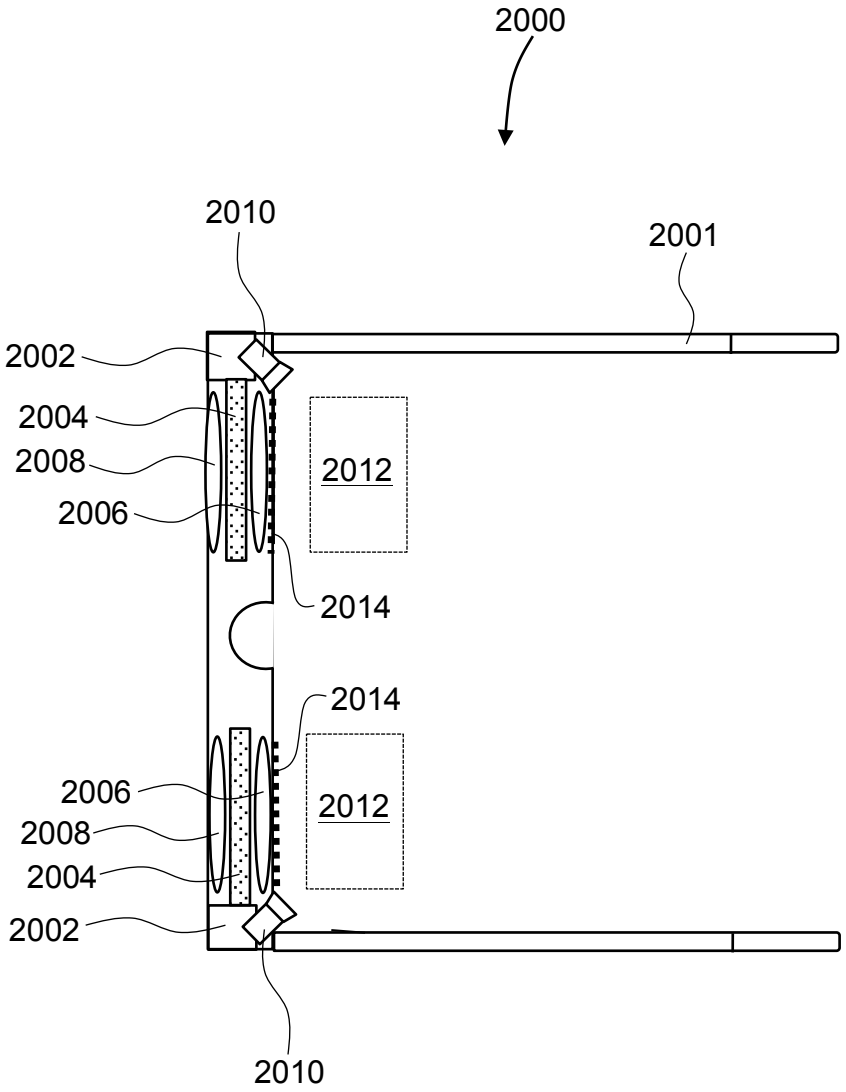
2000
2010
2001
2002
2004
2008
2006
2012
2014
2014
2006
2008
2004
2012
2002
2010

FIG. 20

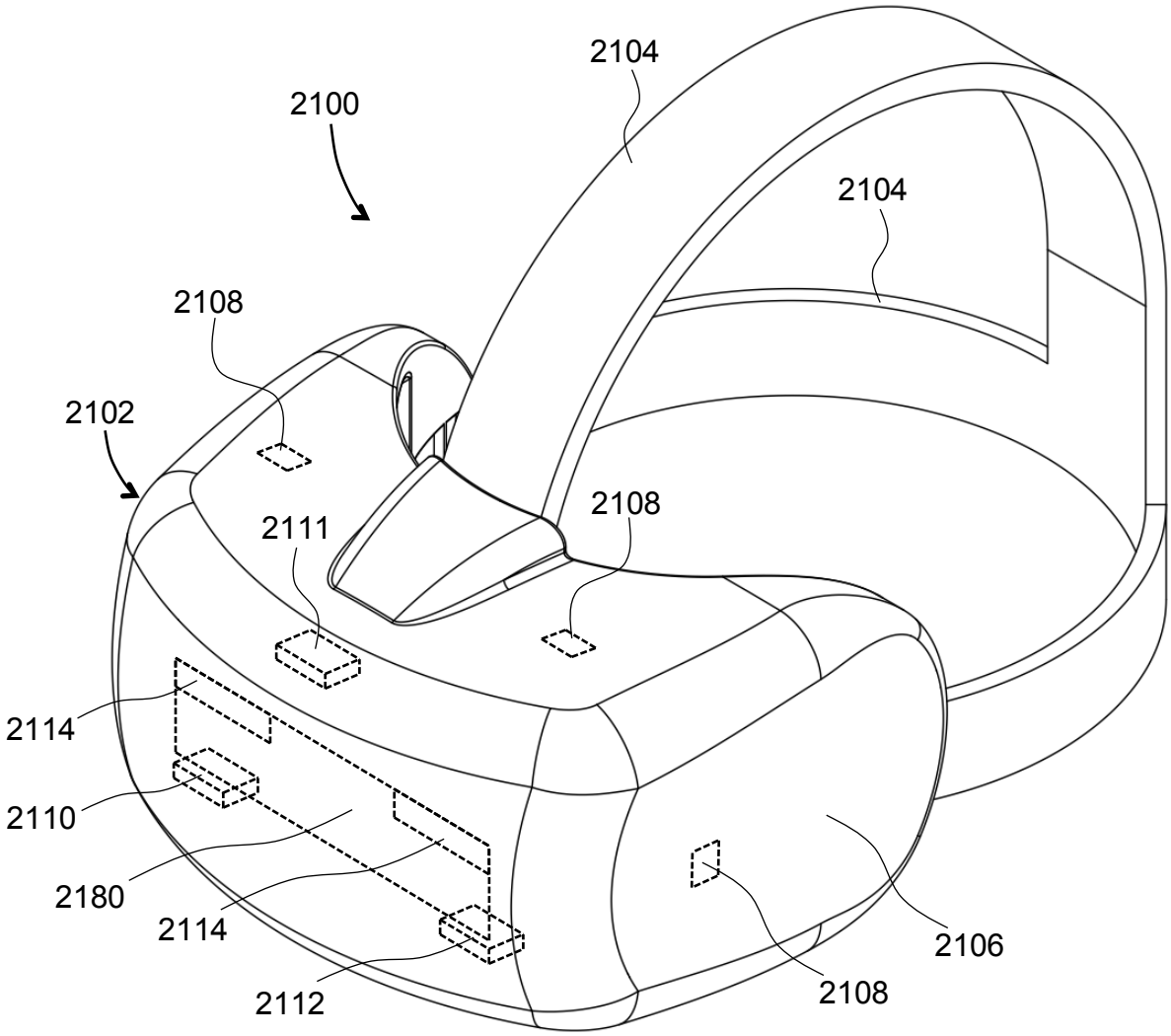
2104
2100
2104
2108
2102
2111
2108
2114
2110
2180
2114
2112
2106
2108

FIG. 21